Dept. of Math. University of Oslo
Mechanics and Applied Mathematics No. 1
ISSN 0809–4403 May 2009

NEW CURRENT MODIFIED SCHRÖDINGER EQUATIONS

Karina B. Hjelmervik & Karsten Trulsen
Mechanics Division, Department of Mathematics, University of Oslo, Norway

Abstract

New current modified Schrödinger equations are derived suited to study waves on both potential and non–potential inhomogeneous currents. Split–step schemes of first, second, and fourth order are discussed. Different results are presented regarding the current terms and the model setup.

This paper mainly serve as background information for Hjelmervik & Trulsen (2009), but the current modified Schrödinger equations and model setup presented here are expected to have an even larger range of application possibilities.

1 Introduction

Studies of nonlinear wave–current interactions are of academic interest and important in order to reduce safety hazards in ocean currents.

Even linear interaction of waves and currents is still an active field of research. It is well known that linear refraction due to currents can provoke large waves. Waves encountering an opposing current may obtain reduced wave length and increased wave height and steepness. When waves encounter an opposing current jet, focusing can further enhance the wave intensity near the centre of the jet. Linear refraction of waves by currents is known to cause navigational problems, e.g. in the Agulhas current, river estuaries, rip currents, entrances in fjords during outgoing tides, and in tidal flows in the coastal zone, (Longuet-Higgins & Stewart, 1961; Peregrine, 1976; González, 1984; Jonsson, 1990; Lavrenov, 1998; Bottin & Thompson, 2002; Mori, Liu & Yasuda, 2002; MacIver, Simons & Thomas, 2006; MacMahan, Thornton & Reniers, 2006). When the steepness thus increases, enhanced nonlinear modulations is anticipated (Stocker & Peregrine, 1999; Lavrenov & Porubov,

2006). However, it is not well known how the enhanced effect of nonlinearity modify the wave height. Our goal is to investigate how current and nonlinearity modifies the wave heights for waves propagating on inhomogeneous stationary currents. In this paper we will derive equations and construct a numerical setup for this purpose. We will also study some results regarding the model setup, the current terms, and different current configurations.

Several different equations are used to study wave–current interactions. Our need to resolve wave phases on non–potential currents restricts us from employing several obvious candidates. White (1999) allowed a prescribed current with vorticity, and derived a wave action equation which is a phase averaged model. Ray theory (White & Fornberg, 1998) is used for tracking wave packets. Peregrine & Smith (1979) derived a nonlinear Schrödinger equation useful for caustics where ray theory breaks down. Schrödinger equations have bandwidth constraints which may be problematic. The Zakharov (1968) equation does not have bandwidth constraints, but makes it hard to include a prescribed current, and is limited to potential flows.

Here we derive a current modified cubic Schrödinger equation suited for waves on prescribed, stationary collinear currents. Some related models have already been published. Stewartson (1977) considered the effects of slowly varying depth and current, and derived a cubic Schrödinger equation limiting to potential theory. Turpin, Benmoussa & Mei (1983) considered the effects of slowly varying depth and current, and derived a cubic Schrödinger equation limiting to one horizontal dimension. Gerber (1987) used the variational principle to derive a cubic Schrödinger equation for a non–uniform medium, limiting to potential theory in one horizontal dimension. Stocker & Peregrine (1999) extended the modified nonlinear Schrödinger equation of Dysthe (1979) to include a slowly varying, periodic current and derived a current modified Schrödinger equation. As an application example of their theory, they studied the effect on a wave field from a potential surface current induced by an internal wave. Their dominant current term, UB, is of cubic order. We want to study stronger currents. Our equation will be taken up to cubic nonlinearity, and will include waves and currents in two horizontal dimensions allowing horizontal shear.

Several methods may be used to derive nonlinear Schrödinger equations for deep water waves: an averaged Lagrangian method (Yuen & Lake, 1982), a spectral method (Zakharov, 1968), and a multiple scales method (Hasimoto & Ono, 1972; Davey & Stewartson, 1974; Dysthe, 1979; Stocker & Peregrine, 1999). We have used a multiple scale expansion similar to Mei (1989).

Several numerical methods may be used to solve nonlinear Schrödinger equations. We employ a split–step method using both Fourier methods and finite difference methods (Lo & Mei, 1985; Weidman & Herbst, 1986; Stocker

& Peregrine, 1999). The Fourier methods are used on the linear terms with constant coefficients. The finite difference methods are used on the nonlinear terms and the linear terms with variable coefficients. Lo & Mei (1985) used a split–step scheme to solve the modified Schrödinger equation by Dysthe and compared their results with experiments.

2 Wave paths on prescribed currents

The linear dispersion relation for gravity waves on deep water is given by:

$$(\omega - \mathbf{k} \cdot \mathbf{U})^2 \quad = \quad gk \tag{1}$$

$\omega = \omega(k_x, k_y, x, y, t)$ is the angular frequency. $g = 9.81\text{m/s}^2$ is the acceleration of gravity. $\mathbf{k} = k_x\mathbf{i} + k_y\mathbf{j}$ is the wave vector with wave number $k = \sqrt{k_x^2 + k_y^2}$. And $\mathbf{U} = U(x, y)\mathbf{i} + V(x, y)\mathbf{j}$ is the horizontal surface current which is assumed stationary and slowly varying spatially. Since $\boldsymbol{U}$ is the horizontal surface current, it does not have to be divergence free. The full current field has a vertical component which does not appear in the dispersion relation (1).

(1) may be made dimensionless using the characteristic length and time scales of the wave field in the absence of current:

$$(\omega - \mathbf{k} \cdot \mathbf{U})^2 \quad = \quad k \tag{2}$$

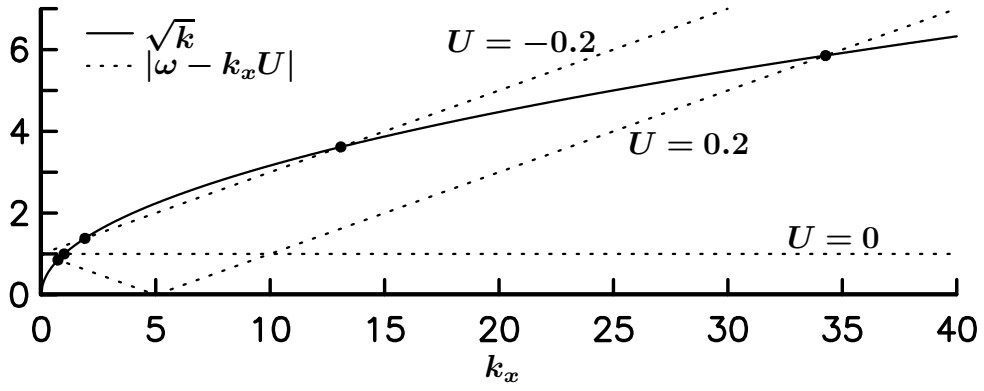

Figure 1: *The dimensionless linear dispersion relation (2) for long crested gravity waves,* $\mathbf{k} = k_x\boldsymbol{i}$*, on a collinear current,* $\boldsymbol{U} = U(x)\boldsymbol{i}$*. Here* $\omega = 1$*. Solutions for selected currents are marked with disks.*

There are up to four solutions of (2) for long crested waves, $\boldsymbol{k} = k_x\boldsymbol{i}$, on a collinear current, $\boldsymbol{U} = U(x)\boldsymbol{i}$, (figure 1 and 2). There exist only two

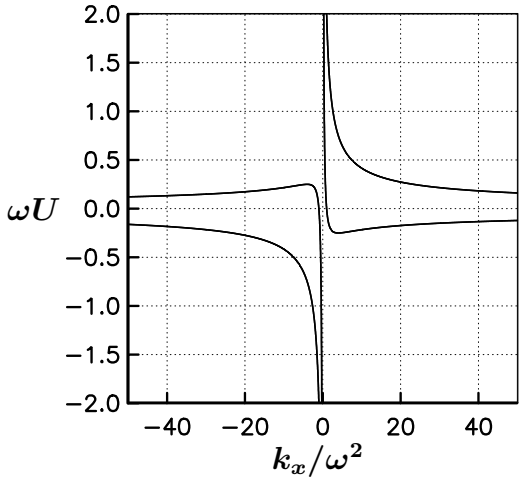

Figure 2: *The linear dispersion relation (2) for long crested gravity waves,* $\mathbf{k} = k_x\boldsymbol{i}$*, on a collinear current,* $\boldsymbol{U} = U(x)\boldsymbol{i}$*. Both coordinate axes are asymptotes for all curves.* $\omega^2 = \pm k_x$ *when* $U = 0$*. A local minimum is found in* $(k_x/\omega^2, \omega U) = (4, -0.25)$*.*

solutions when $U = 0$ or $|U| > \frac{1}{4\omega}$, three solutions when $|U| = \frac{1}{4\omega}$, and four solutions when $|U| < \frac{1}{4\omega}$.

Without any current the solutions are $\omega = \pm\sqrt{k}$, depending on the direction of the waves. If the waves encounter a co–current ($k_xU > 0$), the wavelength increases. If the waves encounter a counter current ($k_xU < 0$), the wavelength decreases. In both cases the phase velocity of the waves is stronger than the group velocity of the waves.

When $U = -\frac{1}{4\omega}\frac{k_x}{k}$, the group velocity of the waves has the same strength as the velocity of the counter current. If the counter current increases further in strength, there does not exist any solution of the dispersion relation because the energy of the waves cannot propagate on such strong counter currents. If the counter current decreases in strength, the wave train may split in two parts with decreasing and increasing wave number respectively. With decreasing wave number the phase velocity of the waves is stronger than the group velocity of the waves, and as the strength of the counter current approaches zero, the wave number approaches ω^2. With increasing wave number the group velocity follows the counter current. As the strength of the counter current approaches zero, the wave number approaches infinity.

On a co–current there exist solutions with high wave numbers which increase when the strength of the co–current decrease. The group velocity is larger than the phase velocity. This situation cannot be provoked by the current, but if provoked it can exist on a current. When the wave number exceeds a certain threshold, the capillary waves are more dominant than the gravity waves, see Trulsen & Mei (1993)

2.1 Wave path equations

The wave paths are tangential with the group velocity, $\boldsymbol{c}_g$, while the rays are tangential with the wave number vector, $\boldsymbol{k}$. Since the dispersion relation (2) is not isotropic, the wave paths and the rays do not coincide. The wave path equations may be written by:

$$\frac{\mathrm{d}\omega}{\mathrm{d}t} = \frac{\partial \omega}{\partial t} = 0 \tag{3}$$

$$\frac{\mathrm{d}\mathbf{k}}{\mathrm{d}t} = -\frac{\partial \omega}{\partial \mathbf{x}} = -k_x \left(\frac{\partial U}{\partial x}\boldsymbol{i} + \frac{\partial U}{\partial y}\boldsymbol{j} \right) \tag{4}$$

$$\frac{\mathrm{d}\mathbf{x}}{\mathrm{d}t} = \frac{\partial \omega}{\partial \mathbf{k}} = \mathbf{U} \pm \frac{1}{2\sqrt{k}}\frac{\mathbf{k}}{k} \tag{5}$$

Here the x-axis is aligned along the current so that $\boldsymbol{U} = U(x,y)\boldsymbol{i}$.

According to (3) the angular frequency, ω, is constant for each wave path. Suppose that $U = U_0$ and $\boldsymbol{k} = (k_{x0}, k_{y0})$ at $x = x_0$. The conserved frequency will then be:

$$\omega = k_{x0}U_0 \pm \left(\sqrt{k_{x0}^2 + k_{y0}^2} \right)^{1/2} \tag{6}$$

The wave paths are longitudinally reflected when $U \pm \frac{1}{2\sqrt{k}}\frac{k_x}{k} = 0$ and transversally reflected when $k_y = 0$ according to (5). Suppose that $U = U_{Rl}$ when the wave paths are longitudinally reflected, and $U = U_{Rt}$ when the wave paths are transversally reflected. If $k_{y0} = 0$, U_{Rl} and U_{Rt} are given by:

$$U_{Rl} = -\frac{1}{4\omega} \tag{7}$$

$$U_{Rt} = U_0 \tag{8}$$

The stopping velocity in (7) is in agreement with Peregrine (1976), White & Fornberg (1998), and others.

Following Mei (1989) it can be shown that B satisfies the following conservation law:

$$\frac{\partial}{\partial t}\left(\frac{B^2}{\sigma} \right) + \nabla_h \cdot \left(\mathbf{c_g} \frac{B^2}{\sigma} \right) = 0 \tag{9}$$

B is the amplitude of the waves. σ and $\mathbf{c}_g$ are given by:

$$\sigma = \omega - \mathbf{U} \cdot \mathbf{k}$$

$$\mathbf{c}_g = \mathbf{U} \pm \frac{1}{2\sqrt{k}}\frac{\mathbf{k}}{k}$$

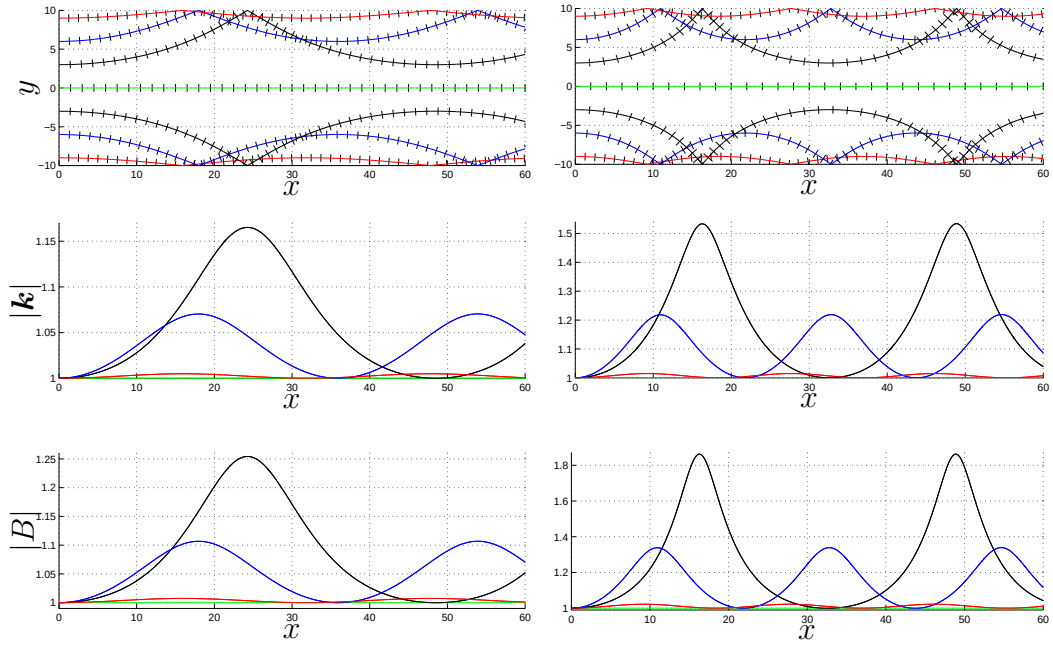

(a) $U_0 = 0.1$ (b) $U_0 = 0.3$

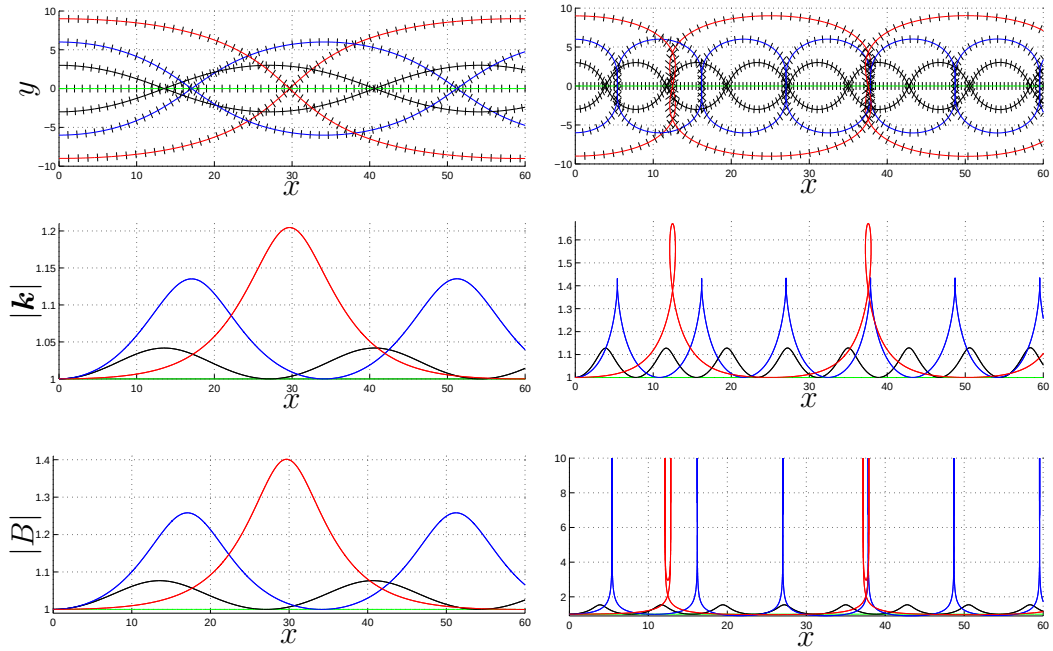

(c) $U_0 = -0.1$ (d) $U_0 = -0.3$

Figure 3: *Wave paths with corresponding wave number,* $|\boldsymbol{k}|$*, and amplitude,* $|B|$*, as a function of* x *according to (3)–(5) and (9). The short lines across the wave paths are normal to the wave vector* $\boldsymbol{k}$*. Here* $\omega = 1$*.*

(9) may also be written on the same form as the wave path equations, in order to calculate the amplitude while tracing a path:

$$\frac{\mathrm{d}}{\mathrm{d}t}\left(\frac{B^2}{\sigma}\right) = \frac{\partial}{\partial t}\left(\frac{B^2}{\sigma}\right) + \mathbf{c}_g \cdot \nabla_h \left(\mathbf{c_g}\frac{B^2}{\sigma}\right) = -\left(\frac{B^2}{\sigma}\right)\nabla \cdot \mathbf{c}_g \qquad (10)$$

2.1.1 An example

Suppose that the waves ride a collinear current jet where $\mathbf{U} = U(y)\mathbf{i}$:

$$U(y) = U_0 \cos^2\left(\frac{\pi y}{Y}\right) \qquad (11)$$

The rays diverge on co–currents (figure 3a–b) and converge on counter currents (figure 3c–d). The rays are transversally reflected at the same velocity as the initial velocity in agreement with (8). Since the dispersion relation (2) is not isotropic, the wave vector, $\boldsymbol{k}$, is not tangential with the wave paths except when the wave vector is parallel to the current, $\boldsymbol{U}$.

On co–current jets the amplitude and wave number increase towards the channel walls and decrease towards the centre of the jet. On counter current jets the amplitude and wave number increase towards the centre of the jet. When the counter current is stronger than the stopping velocity, (7), the rays are reflected longitudinally (figure 3d).

2.2 Exact dispersion for constant current

Suppose that only the positive root is applied in (2):

$$\omega = k_x U + k_y V + \left(k_x^2 + k_y^2\right)^{\frac{1}{4}} \qquad (12)$$

Let $\omega = 1 + \triangle\omega$ and $\boldsymbol{k} = (k_x, k_y) = (1 + \triangle k_x, \triangle k_y)$ where $\triangle\omega$ is the modulation frequency and $(\triangle k_x, \triangle k_y)$ is the modulation wave vector:

$$1 + \triangle\omega = (1 + \triangle k_x)U + \triangle k_y V + \left(1 + 2\triangle k_x + (\triangle k_x)^2 + (\triangle k_y)^2\right)^{\frac{1}{4}} \qquad (13)$$

Taylor expansion of the last term gives:

$$\triangle\omega - U - \triangle k_x U - \triangle k_y V - \frac{1}{2}\triangle k_x + \frac{1}{8}(\triangle k_x)^2 - \frac{1}{4}(\triangle k_y)^2 - \frac{1}{16}(\triangle k_x)^3 + \frac{3}{8}\triangle k_x(\triangle k_y)^2 = O\left((\triangle k)^4\right) \qquad (14)$$

Following the method of Yuen & Lake (1982) and Trulsen *et al.* (2000), (14) may then be transformed using the following direct correspondences:

$$\triangle\omega \rightarrow i\frac{\partial}{\partial t}, \qquad \triangle k_x \rightarrow -i\frac{\partial}{\partial x}, \qquad \triangle k_y \rightarrow -i\frac{\partial}{\partial y} \tag{15}$$

For a linear, homogeneous wave system of uniform properties these correspondences can be made rigorous. When including inhomogeneous currents, the two last relationships in (15) are not accurate unless the $\nabla \boldsymbol{U}$–terms can be neglected (Stocker & Peregrine, 1999).

Suppose that the current is slowly varying so that the waves do not feel the changes locally. Then the relations in (15) used on (14) give:

$$\begin{aligned} i\frac{\partial}{\partial t} - U + iU\frac{\partial}{\partial x} + iV\frac{\partial}{\partial y} + \frac{i}{2}\frac{\partial}{\partial x} - \frac{1}{8}\frac{\partial^2}{\partial x^2} + \frac{1}{4}\frac{\partial^2}{\partial y^2} \\ -\frac{i}{16}\frac{\partial^3}{\partial x^3} + \frac{3i}{8}\frac{\partial^3}{\partial x \partial y^2} = O\left((\triangle k)^4\right) \end{aligned} \tag{16}$$

If multiplied with $-iB$, the linear terms in a time evolution of a current modified Scrödinger equation appear:

$$\begin{aligned} \frac{\partial B}{\partial t} + \frac{1}{2}\frac{\partial B}{\partial x} + iUB + U\frac{\partial B}{\partial x} + V\frac{\partial B}{\partial y} + \frac{i}{8}\frac{\partial^2 B}{\partial x^2} - \frac{i}{4}\frac{\partial^2 B}{\partial y^2} \\ -\frac{1}{16}\frac{\partial^3 B}{\partial x^3} + \frac{3}{8}\frac{\partial^3 B}{\partial x \partial y^2} = O\left((\triangle k)^4\right) \end{aligned} \tag{17}$$

In the next section, current modified nonlinear Schrödinger equations will be derived using multiple scales. These equations will allow inhomogeneous currents.

3 Evolution of current modified nonlinear Schrödinger equations

Assume that the total velocity field, $\boldsymbol{v}_{tot} = \boldsymbol{v} + \boldsymbol{V}$, is a superposition of the velocity of a wave field, $\boldsymbol{v} = (u, v, w)$, and a prescribed stationary current field, $\boldsymbol{V} = (U, V, W)$, in a Cartesian coordinate system, (x, y, z). The x–axis is aligned with the principal propagation direction of the waves. The z–axis is vertical with unit vector $\boldsymbol{k}$ pointing upwards. $z = 0$ corresponds to the undisturbed free water surface. The water is assumed inviscid, incompressible, and deep with respect to the characteristic wavelength. The current field is assumed unaffected by waves. η and ζ are the surface displacements associated with the wave field and the current field respectively.

	Potential current (sec. 3.1)	Vorticity allowed (sec. 3.2)	Stewartson (1977)	Stocker & Peregrine (1999)	Hjelmervik & Trulsen (2009)
ak_c	ϵ	ϵ	0	ϵ	ϵ
$(U,V)k_c/\omega_c$	ϵ	ϵ	1	ϵ^2	ϵ
Wk_c/ω_c	ϵ^5	ϵ^4	ϵ^2	ϵ^2	ϵ^2
Ak_c	ϵ^2	ϵ^2	0	ϵ^2	ϵ^2
$1/k_cX$	ϵ^2	ϵ	ϵ	ϵ	ϵ
$1/k_cY$	ϵ^2	1	ϵ	ϵ	ϵ
$1/\omega_cT$	0	0	ϵ^2	ϵ	0
Nonlinear	yes	yes	no	yes	yes
Horizontal dimensions	2	2	2	2	2
Potential theory	yes	no	yes	yes	no

Table 1: *Current modified Schrödinger equations. k_c and ω_c are the characteristic wave number and frequency for the undisturbed wave field, $\omega_c^2 = gk_c$. a and A are the amplitudes associated with the wave field and the surface current field respectively. (U,V,W) is the characteristic current with a characteristic length scale (X,Y,Z) and time scale T.*

The Euler equation for the combined wave and current field can be written as:

$$\frac{\partial \boldsymbol{v}}{\partial t} + \boldsymbol{v}_{tot} \cdot \boldsymbol{\nabla} \boldsymbol{v}_{tot} = -\frac{1}{\rho} \boldsymbol{\nabla} p_{tot} - g\boldsymbol{k} \tag{18}$$

The total pressure, $p_{tot} = p + P + p_s$, is a combination of the dynamic pressure due to the wave field, p, the dynamic pressure due to the current field, P, and the static pressure, $p_s = p_a - \rho g z$, where p_a is the atmospheric pressure, ρ is the density, and g is the acceleration of gravity.

The vorticity of the waves, $\boldsymbol{\gamma} = \boldsymbol{\nabla} \times \boldsymbol{v}$, obeys the equation:

$$\frac{\partial \boldsymbol{\gamma}}{\partial t} + \boldsymbol{v}_{tot} \cdot \boldsymbol{\nabla} \boldsymbol{\gamma} - \boldsymbol{\gamma} \cdot \boldsymbol{\nabla} \boldsymbol{v}_{tot} = -\boldsymbol{v} \cdot \boldsymbol{\nabla} \boldsymbol{\Gamma} + \boldsymbol{\Gamma} \cdot \boldsymbol{\nabla} \boldsymbol{v} \tag{19}$$

If the vorticity of the current, $\boldsymbol{\Gamma} = \boldsymbol{\nabla} \times \boldsymbol{V}$, equals zero, (19) is homogeneous with respect to $\boldsymbol{\gamma}$, and if the wave field starts out irrotational, it will remain irrotational. For waves riding a current field with vorticity, vorticity will develop in the wave field as well.

Traditional Schrödinger equations are built on potential theory (Davey & Stewartson, 1974; Stewartson, 1977; Dysthe, 1979; Dysthe & Das, 1981;

Gerber, 1987; Stocker & Peregrine, 1999; Trulsen *et al.*, 2000). Here we will derive two current modified nonlinear Schrödinger equations. The first is built on potential theory (sec. 3.1), and the second allows horizontal shear and includes all the terms from the first (sec. 3.2). In table 1 the characteristic sizes of these derivations are compared to some of the derivations found in literature.

Let a, k_c and ω_c be the characteristic amplitude, wavenumber and angular frequency of the surface waves. We employ the steepness of the waves as a small ordering parameter in the following, $\epsilon = ak_c \ll 1$, thus $k_c\eta = O(\epsilon)$ and $\boldsymbol{v}\frac{k_c}{\omega_c} = O(\epsilon)$. The horizontal current velocities are assumed just small enough to avoid collinear reflection of the waves, $(U,V)\frac{k_c}{\omega_c} = O(\epsilon)$. The vertical surface current velocity is assumed negligible, $W\frac{k_c}{\omega_c} = O(\epsilon^5)$ when potential theory is used, and $W\frac{k_c}{\omega_c} = O(\epsilon^4)$ when vorticity is allowed. It follows from the Bernoulli equation that the surface displacement induced by the current is small, $Ak_c = O(\epsilon^2)$.

3.1 Potential current field

If the current field is a potential field, $\boldsymbol{V} = \boldsymbol{\nabla}\Phi$, the velocity of the wave field can be represented by a potential, $\boldsymbol{v} = \boldsymbol{\nabla}\phi$, according to (19).

The continuity equation for the wave field, may be written as:

$$\boldsymbol{\nabla}^2\phi \;=\; 0 \tag{20}$$

The waves are assumed on deep water, that is $\nabla\phi \to 0$ as $z \to -\infty$. The surface equations for the combined field at the free surface $z = \eta + \zeta$, can be written as:

$$\frac{\partial\eta}{\partial t} + \boldsymbol{\nabla}(\phi+\Phi)\cdot\boldsymbol{\nabla}(\eta+\zeta) \;=\; \frac{\partial}{\partial z}(\phi+\Phi) \tag{21}$$

$$\frac{\partial\phi}{\partial t} + \frac{1}{2}\left(\boldsymbol{\nabla}(\phi+\Phi)\right)^2 + g(\eta+\zeta) \;=\; 0 \tag{22}$$

Taylor expansions around $z = 0$ gives (21–22) on the form:

$$\begin{aligned}
&\frac{\partial\eta}{\partial t} + \nabla\phi\cdot\nabla(\eta+\zeta) + \nabla\Phi\cdot\nabla\eta + \zeta\nabla\frac{\partial}{\partial z}(\phi+\Phi)\cdot\nabla\eta + \zeta\nabla\frac{\partial\phi}{\partial z}\cdot\nabla\zeta \\
&\quad + \eta\nabla\frac{\partial}{\partial z}(\phi+\Phi)\cdot\nabla(\eta+\zeta) + \frac{1}{2}\eta(\eta+2\zeta)\nabla\frac{\partial}{\partial z}(\phi+\Phi)\cdot\nabla(\eta+\zeta) \\
&\quad + \frac{1}{2}\zeta^2\nabla\frac{\partial}{\partial z}(\phi+\Phi)\cdot\nabla\eta + \frac{1}{2}\zeta^2\nabla\frac{\partial\phi}{\partial z}\cdot\nabla\zeta + \frac{1}{6}\eta^3\nabla\frac{\partial^2\phi}{\partial z}\cdot\nabla\eta \\
&\quad = \frac{\partial\phi}{\partial z} + \eta\frac{\partial^2}{\partial z^2}(\phi+\Phi) + \zeta\frac{\partial^2\phi}{\partial z^2} + \frac{1}{2}\eta(\eta+2\zeta)\frac{\partial^3}{\partial z^3}(\phi+\Phi) + \frac{1}{2}\zeta^2\frac{\partial^3\phi}{\partial z^3}
\end{aligned}$$

$$+\frac{1}{6}\eta^3\frac{\partial^4\phi}{\partial z^4}+\cdots \tag{23}$$

$$\frac{\partial\phi}{\partial t}+(\eta+\zeta)\frac{\partial^2\phi}{\partial t\partial z}+\frac{1}{2}(\eta+\zeta)^2\frac{\partial^3\phi}{\partial t\partial z^2}+\frac{1}{6}(\eta+\zeta)^3\frac{\partial^4\phi}{\partial t\partial z^3}$$
$$+\frac{1}{2}\nabla\phi\cdot\nabla(\phi+2\Phi)+\eta\nabla(\phi+\Phi)\cdot\nabla\frac{\partial}{\partial z}(\phi+\Phi)+\zeta\nabla(\phi+\Phi)\cdot\nabla\frac{\partial\phi}{\partial z}$$
$$+\zeta\nabla\phi\cdot\nabla\frac{\partial\Phi}{\partial z}+\frac{1}{2}\eta^2\left(\nabla\frac{\partial\phi}{\partial z}\right)^2+\frac{1}{2}\eta^2\nabla\phi\cdot\nabla\frac{\partial^2\phi}{\partial z^2}+g\eta+\cdots=0 \tag{24}$$

Let the horizontal length scales, L, of the current be longer than a characteristic wavelength so that $1/(k_cL)=O(\epsilon^2)$. In accordance with the scaling assumptions, all equations, variables, and sizes in the following are made dimensionless using the characteristic length and time scales of the wave field, so that $k_c\boldsymbol{x}\to\boldsymbol{x}$, $\epsilon k_c\boldsymbol{x}\to\bar{\boldsymbol{x}}$, $\omega_c t\to t$, $k_c\eta\to\epsilon\eta$, $k_c\zeta\to\epsilon^2\zeta$, $\frac{1}{\omega_c}\phi\to\epsilon\phi$, $\frac{k_c}{\omega_c}(U,V)\to\epsilon(U,V)$, and $\frac{k_c}{\omega_c}W\to\epsilon^5 W$,

The wave field is represented by perturbation series for the surface displacement, η, and the velocity potential, ϕ:

$$\begin{aligned}\eta=&\ \epsilon\bar{\eta}+\tfrac{1}{2}\Big(B_1\mathrm{e}^{\mathrm{i}(x-t)}+\epsilon B_2\mathrm{e}^{2\mathrm{i}(x-t)}+\epsilon^2B_3\mathrm{e}^{3\mathrm{i}(x-t)}+\cdots+\text{c.c.}\Big)\\ \phi=&\ \epsilon\bar{\phi}+\tfrac{1}{2}\Big(A_1'\mathrm{e}^{\mathrm{i}(x-t)}+\epsilon A_2'\mathrm{e}^{2\mathrm{i}(x-t)}+\epsilon^2A_3'\mathrm{e}^{3\mathrm{i}(x-t)}+\cdots+\text{c.c.}\Big)\end{aligned} \tag{25}$$

$\bar{\eta}=\bar{\eta}(\bar{x},\bar{y},\bar{t})$ and $\bar{\phi}=\bar{\phi}(\bar{x},\bar{y},z,\bar{t})$ are the mean surface displacement and mean induced velocity potential respectively. $B_n=B_n(\bar{x},\bar{y},\bar{t})$ and $A_n'=A_n'(\bar{x},\bar{y},z,\bar{t})$ are the n'th harmonics of the surface displacement and the induced current potential respectively. The characteristic wavenumber is fixed appropriate for waves undisturbed by current, therefore the entire effect of refraction is represented by modulations of B_1.

Both the mean functions and the harmonics, are perturbed:

$$\begin{aligned}\bar{\eta}&=\bar{\eta}_1+\epsilon\bar{\eta}_2+\cdots, & B_n&=B_{n0}+\epsilon B_{n1}+\epsilon^2B_{n2}+\cdots\\ \bar{\phi}&=\bar{\phi}_1+\epsilon\bar{\phi}_2+\cdots, & A_n'&=A_{n0}'+\epsilon A_{n1}'+\epsilon^2A_{n2}'+\cdots\end{aligned} \tag{26}$$

3.1.1 Vertical dependence

The n'th harmonic terms of the scaled continuity equation, (20) is given by:

$$\frac{\partial^2A_n'}{\partial z^2}-n^2A_n'+2\epsilon\mathrm{i}n\frac{\partial^2A_n'}{\partial\bar{x}}+\epsilon^2\left(\frac{\partial^2A_n'}{\partial\bar{x}^2}+\frac{\partial^2A_n'}{\partial\bar{y}^2}\right)\ =\ 0 \tag{27}$$

where $\frac{\partial A_n'}{\partial z}\to 0$ as $z\to-\infty$.

First order To first order the continuity equation for A'_n (27) is:

$$\frac{\partial^2 A'_{n0}}{\partial z^2} - n^2 A'_{n0} = 0 \tag{28}$$

which has the solution:

$$A'_{n0} = A_{n0}(\bar{x}, \bar{y}, \bar{t})\mathrm{e}^{nz} \tag{29}$$

since $\frac{\partial A'_{n0}}{\partial z} \to 0$ as $z \to -\infty$.

Second order To second order the continuity equation for A'_n (27) is:

$$\frac{\partial^2 A'_{n1}}{\partial z^2} - n^2 A'_{n1} + 2\mathrm{i}n\frac{\partial A'_{n0}}{\partial \bar{x}} = 0 \tag{30}$$

where $\frac{\partial A'_{n1}}{\partial z} \to 0$ as $z \to -\infty$.

Using the result from first order (29), gives:

$$\frac{\partial^2 A'_{n1}}{\partial z^2} - n^2 A'_{n1} + 2\mathrm{i}n\frac{\partial A_{n0}}{\partial \bar{x}}\mathrm{e}^{nz} = 0 \tag{31}$$

which has the solution:

$$A'_{n1} = A_{n1}(\bar{x}, \bar{y}, \bar{t})\mathrm{e}^{nz} - \mathrm{i}\frac{\partial A_{n0}}{\partial \bar{x}}z\mathrm{e}^{nz} \tag{32}$$

Third order To third order the continuity equation for A'_n (27) is:

$$\frac{\partial^2 A'_{n2}}{\partial z^2} - n^2 A'_{n2} + 2\mathrm{i}n\frac{\partial A'_{n1}}{\partial \bar{x}} + \frac{\partial^2 A'_{n0}}{\partial \bar{x}^2} + \frac{\partial^2 A'_{n0}}{\partial \bar{y}^2} = 0 \tag{33}$$

where $\frac{\partial A'_{n2}}{\partial z} \to 0$ as $z \to -\infty$.

Using the results from first and second order (29, 32) gives:

$$\frac{\partial^2 A'_{n2}}{\partial z^2} - n^2 A'_{n2} + 2\mathrm{i}n\frac{\partial A_{n1}}{\partial \bar{x}} + \frac{\partial^2 A_{n0}}{\partial \bar{x}^2}(1 + 2nz)\mathrm{e}^{nz} + \frac{\partial^2 A_{n0}}{\partial \bar{y}^2}\mathrm{e}^{nz} = 0 \tag{34}$$

which has the solution:

$$A'_{n2} = A_{n2}(\bar{x}, \bar{y}, \bar{t})\mathrm{e}^{nz} - \mathrm{i}\frac{\partial A_{n1}}{\partial \bar{x}}z\mathrm{e}^{nz} - \frac{1}{2n}\frac{\partial^2 A_{n0}}{\partial \bar{y}^2}z\mathrm{e}^{nz} - \frac{1}{2}\frac{\partial^2 A_{n0}}{\partial \bar{x}^2}z^2\mathrm{e}^{nz} \tag{35}$$

Fourth order To fourth order the continuity equation for A'_n (27) is:

$$\frac{\partial^2 A'_{n3}}{\partial z^2} - n^2 A'_{n3} + 2\mathrm{i}n\frac{\partial A'_{n2}}{\partial \bar{x}} + \frac{\partial^2 A'_{n1}}{\partial \bar{x}^2} + \frac{\partial^2 A'_{n1}}{\partial \bar{y}^2} = 0 \tag{36}$$

where $\frac{\partial A'_{n3}}{\partial z} \to 0$ as $z \to -\infty$.

Using the result from first, second, and third order (29, 32, 35) gives:

$$\begin{aligned}\frac{\partial^2 A'_{n3}}{\partial z^2} - n^2 A'_{n3} + 2\mathrm{i}n\frac{\partial A_{n2}}{\partial \bar{x}} + \frac{\partial^2 A_{n1}}{\partial \bar{x}^2}(1+2nz)\mathrm{e}^{nz} + \frac{\partial^2 A_{n1}}{\partial \bar{y}^2}\mathrm{e}^{nz} \\ -2\mathrm{i}\frac{\partial^3 A_{n0}}{\partial \bar{x}\partial \bar{y}^2}z\mathrm{e}^{nz} - \mathrm{i}\frac{\partial^3 A_{n1}}{\partial \bar{x}^3}z(1+nz)\mathrm{e}^{nz} &= 0\end{aligned} \tag{37}$$

which has the solution:

$$\begin{aligned}A'_{n3} &= A_{n3}(\bar{x},\bar{y},\bar{t})\mathrm{e}^{nz} - \mathrm{i}\frac{\partial A_{n2}}{\partial \bar{x}}z\mathrm{e}^{nz} - \frac{1}{2n}\frac{\partial^2 A_{n1}}{\partial \bar{y}^2}z\mathrm{e}^{nz} - \frac{1}{2}\frac{\partial^2 A_{n1}}{\partial \bar{x}^2}z^2\mathrm{e}^{nz} \\ &\quad -\frac{\mathrm{i}}{2n^2}\frac{\partial^3 A_{n0}}{\partial \bar{x}\partial \bar{y}^2}z(1-nz)\mathrm{e}^{nz} + \frac{\mathrm{i}}{6}\frac{\partial^3 A_{n0}}{\partial \bar{x}^3}z^3\mathrm{e}^{nz}\end{aligned} \tag{38}$$

Defines $A_n = A_{n0} + \epsilon A_{n1} + \epsilon^2 A_{n2} + \cdots$ which gives:

$$\begin{aligned}A'_n &= A_n\mathrm{e}^{nz} - \mathrm{i}\epsilon\frac{\partial A_n}{\partial \bar{x}}z\mathrm{e}^{nz} - \epsilon^2\left(\frac{1}{2n}\frac{\partial^2 A_n}{\partial \bar{y}^2}z + \frac{1}{2}\frac{\partial^2 A_n}{\partial \bar{x}^2}z^2\right)\mathrm{e}^{nz} \\ &\quad +\epsilon^3\left(\frac{\mathrm{i}}{2n^2}\frac{\partial^3 A_n}{\partial \bar{x}\partial \bar{y}^2}z(nz-1) + \frac{\mathrm{i}}{6}\frac{\partial^3 A_n}{\partial \bar{x}^3}z^3\right)\mathrm{e}^{nz} + O(\epsilon^4)\end{aligned} \tag{39}$$

3.1.2 Surface equations

The scaled surface equations (23–24) to the fourth order of ϵ are given by:

$$\begin{aligned}&\frac{\partial \eta}{\partial t} + \epsilon\frac{\partial \phi}{\partial x}\frac{\partial \eta}{\partial x} + \epsilon U\frac{\partial \eta}{\partial x} + \epsilon^2\eta\frac{\partial^2 \phi}{\partial x\partial z}\frac{\partial \eta}{\partial x} + \frac{1}{2}\epsilon^3\eta^2\frac{\partial^3 \phi}{\partial x\partial z^2}\frac{\partial \eta}{\partial x} + \epsilon^3\eta\frac{\partial U}{\partial z}\frac{\partial \eta}{\partial x} \\ &\quad +\epsilon^3\zeta\frac{\partial^2 \phi}{\partial x\partial z}\frac{\partial \eta}{\partial x} + \epsilon\frac{\partial \phi}{\partial y}\frac{\partial \eta}{\partial y} + \epsilon V\frac{\partial \eta}{\partial y} + \epsilon^2\eta\frac{\partial^2 \phi}{\partial y\partial z}\frac{\partial \eta}{\partial y} + \frac{1}{2}\epsilon^3\eta^2\frac{\partial^3 \phi}{\partial y\partial z^2}\frac{\partial \eta}{\partial y} \\ &\quad +\epsilon^3\eta\frac{\partial V}{\partial z}\frac{\partial \eta}{\partial y} + \epsilon^3\zeta\frac{\partial^2 \phi}{\partial y\partial z}\frac{\partial \eta}{\partial y} \\ &\quad = \frac{\partial \phi}{\partial z} + \epsilon\eta\frac{\partial^2 \phi}{\partial z^2} + \epsilon^2\zeta\frac{\partial^2 \phi}{\partial z^2} + \frac{1}{2}\epsilon^2\eta^2\frac{\partial^3 \phi}{\partial z^3} + \epsilon^3\eta\zeta\frac{\partial^3 \phi}{\partial z^3} + \frac{1}{6}\epsilon^3\eta^3\frac{\partial^4 \phi}{\partial z^4} \\ &\quad +O(\epsilon^4) \\ &\frac{\partial \phi}{\partial t} + \epsilon\eta\frac{\partial^2 \phi}{\partial t\partial z} + \epsilon^2\zeta\frac{\partial^2 \phi}{\partial t\partial z} + \frac{1}{2}\epsilon^2\eta^2\frac{\partial^3 \phi}{\partial t\partial z^2} + \epsilon^3\eta\zeta\frac{\partial^3 \phi}{\partial t\partial z^2} + \frac{1}{6}\epsilon^3\eta^3\frac{\partial^4 \phi}{\partial t\partial z^3}\end{aligned} \tag{40}$$

$$
\begin{aligned}
&+\frac{1}{2}\epsilon\left(\frac{\partial\phi}{\partial x}\right)^2+\epsilon U\frac{\partial\phi}{\partial x}+\epsilon^2\eta\frac{\partial\phi}{\partial x}\frac{\partial^2\phi}{\partial x\partial z}+\epsilon^2\eta U\frac{\partial^2\phi}{\partial x\partial z}+\frac{1}{2}\epsilon^3\eta^2\left(\frac{\partial^2\phi}{\partial x\partial z}\right)^2\\
&+\frac{1}{2}\epsilon^3\eta^2\frac{\partial\phi}{\partial x}\frac{\partial^3\phi}{\partial x\partial z^2}+\frac{1}{2}\epsilon^3\eta^2U\frac{\partial^3\phi}{\partial x\partial z^2}+\epsilon^3\eta\frac{\partial\phi}{\partial x}\frac{\partial U}{\partial z}+\epsilon^3\zeta\frac{\partial\phi}{\partial x}\frac{\partial^2\phi}{\partial x\partial z}\\
&+\epsilon^3\zeta U\frac{\partial^2\phi}{\partial x\partial z}+\epsilon^3\eta U\frac{\partial U}{\partial z}+\frac{1}{2}\epsilon\left(\frac{\partial\phi}{\partial y}\right)^2+\epsilon V\frac{\partial\phi}{\partial y}+\epsilon^2\eta\frac{\partial\phi}{\partial y}\frac{\partial^2\phi}{\partial y\partial z}\\
&+\epsilon^2\eta V\frac{\partial^2\phi}{\partial y\partial z}+\frac{1}{2}\epsilon^3\eta^2\left(\frac{\partial^2\phi}{\partial y\partial z}\right)^2+\frac{1}{2}\epsilon^3\eta^2\frac{\partial\phi}{\partial y}\frac{\partial^3\phi}{\partial y\partial z^2}+\frac{1}{2}\epsilon^3\eta^2V\frac{\partial^3\phi}{\partial y\partial z^2}\\
&+\epsilon^3\eta\frac{\partial\phi}{\partial y}\frac{\partial V}{\partial z}+\epsilon^3\zeta\frac{\partial\phi}{\partial y}\frac{\partial^2\phi}{\partial y\partial z}+\epsilon^3\zeta V\frac{\partial^2\phi}{\partial y\partial z}+\epsilon^3\eta V\frac{\partial V}{\partial z}+\frac{1}{2}\epsilon\left(\frac{\partial\phi}{\partial z}\right)^2\\
&+\epsilon^2\eta\frac{\partial\phi}{\partial z}\frac{\partial^2\phi}{\partial z^2}+\epsilon^3\zeta\frac{\partial\phi}{\partial z}\frac{\partial^2\phi}{\partial z^2}+\frac{1}{2}\epsilon^3\eta^2\left(\frac{\partial^2\phi}{\partial z^2}\right)^2+\frac{1}{2}\epsilon^3\eta^2\frac{\partial\phi}{\partial z}\frac{\partial^3\phi}{\partial z^3}+\eta\\
&=O(\epsilon^4) \qquad (41)
\end{aligned}
$$

First order To first order of ϵ the surface equations (40–41) give:

$$B_{10} \;=\; \mathrm{i}A_{10} \qquad (42)$$

Second order The zeroth harmonic terms of second order of ϵ in the dynamic surface equation (41) are:

$$\frac{\mathrm{i}}{4}B_{10}A_{10}^*-\frac{\mathrm{i}}{4}A_{10}B_{10}^*+\frac{1}{2}|A_{10}|^2+\bar{\eta}_1 \;=\; 0 \qquad (43)$$

Using the results from first order (42) gives:

$$\bar{\eta}_1 \;=\; 0 \qquad (44)$$

The first harmonic terms of second order of ϵ in the surface equations (40–41) are:

$$-\frac{\mathrm{i}}{2}B_{11}+\frac{1}{2}\frac{\partial B_{10}}{\partial\bar{t}}+\frac{\mathrm{i}}{2}B_{10}U \;=\; \frac{1}{2}A_{11}-\frac{\mathrm{i}}{2}\frac{\partial A_{10}}{\partial\bar{x}} \qquad (45)$$

$$-\frac{\mathrm{i}}{2}A_{11}+\frac{1}{2}\frac{\partial A_{10}}{\partial\bar{t}}+\frac{\mathrm{i}}{2}A_{10}U+\frac{1}{2}B_{11} \;=\; 0 \qquad (46)$$

Using the result from first order (42) gives the Schrödinger equation to linear order:

$$\frac{\partial A_{10}}{\partial\bar{x}}+2\frac{\partial A_{10}}{\partial\bar{t}}+2\mathrm{i}UA_{10} \;=\; 0 \qquad (47)$$

and

$$B_{11} = \mathrm{i}A_{11} - \frac{\partial A_{10}}{\partial \bar{t}} - \mathrm{i}UA_{10} \tag{48}$$

The second harmonic terms to second order of ϵ of the surface equations (40–41) are:

$$-\mathrm{i}B_{20} - \frac{1}{2}A_{10}B_{10} = A_{20} \tag{49}$$

$$-\mathrm{i}A_{20} - \frac{\mathrm{i}}{4}A_{10}B_{10} + \frac{1}{2}B_{20} = 0 \tag{50}$$

Using the result from first order (42) gives:

$$A_{20} = 0 \tag{51}$$

$$B_{20} = -\frac{1}{2}A_{10}^2 \tag{52}$$

Third order The zeroth harmonic terms to third order of ϵ in the surface equations (40–41) are:

$$\frac{\partial \bar{\eta}_1}{\partial \bar{t}} + \frac{\mathrm{i}}{4}A_{10}\frac{\partial B_{10}^*}{\partial \bar{x}} - \frac{\mathrm{i}}{4}B_{10}\frac{\partial A_{10}^*}{\partial \bar{x}} + \frac{\mathrm{i}}{4}\frac{\partial A_{10}}{\partial \bar{x}}B_{10}^* - \frac{\mathrm{i}}{4}\frac{\partial B_{10}}{\partial \bar{x}}A_{10}^* = \frac{\partial \bar{\phi}_1}{\partial z} \tag{53}$$

$$\begin{aligned}\frac{\partial \bar{\phi}_1}{\partial \bar{t}} &+ \frac{1}{4}B_{10}\frac{\partial A_{10}^*}{\partial \bar{t}} + \frac{\mathrm{i}}{4}B_{10}A_{11}^* - \frac{1}{4}B_{10}\frac{\partial A_{10}^*}{\partial \bar{x}} + \frac{1}{4}\frac{\partial A_{10}}{\partial \bar{t}}B_{10}^* - \frac{\mathrm{i}}{4}A_{11}B_{10}^* \\ &- \frac{1}{4}\frac{\partial A_{10}}{\partial \bar{x}}B_{10}^* + \frac{\mathrm{i}}{4}B_{11}A_{10}^* - \frac{\mathrm{i}}{4}A_{10}B_{11}^* + \frac{1}{2}A_{11}A_{10}^* - \frac{\mathrm{i}}{2}\frac{\partial A_{10}}{\partial \bar{x}}A_{10}^* \\ &+ \frac{1}{2}A_{10}A_{11}^* + \frac{\mathrm{i}}{2}A_{10}\frac{\partial A_{10}^*}{\partial \bar{x}} - \frac{\mathrm{i}}{4}UB_{10}A_{10}^* + \frac{\mathrm{i}}{4}UA_{10}B_{10}^* + \bar{\eta}_2 = 0\end{aligned} \tag{54}$$

Using the results from first and second order (42, 44, 48) gives:

$$\frac{\partial \bar{\phi}_1}{\partial z} = -\frac{\partial |A_{10}|^2}{\partial \bar{t}} \tag{55}$$

$$\bar{\eta}_2 = -\frac{\partial \bar{\phi}_1}{\partial \bar{t}} \tag{56}$$

The first harmonic terms of third order of ϵ in the surface equations (40–41) are:

$$\begin{aligned}-\frac{\mathrm{i}}{2}B_{12} &+ \frac{1}{2}\frac{\partial B_{11}}{\partial \bar{t}} - \frac{1}{2}A_{20}B_{10}^* + \frac{1}{4}B_{20}A_{10}^* + \frac{\mathrm{i}}{2}UB_{11} \\ &+ \frac{1}{2}U\frac{\partial B_{10}}{\partial \bar{x}} + \frac{1}{2}V\frac{\partial B_{10}}{\partial \bar{y}} - \frac{1}{8}|B_{10}|^2A_{10} + \frac{1}{16}B_{10}^2A_{10}^*\end{aligned}$$

$$= \frac{1}{2}A_{12} - \frac{\mathrm{i}}{2}\frac{\partial A_{11}}{\partial \bar{x}} - \frac{1}{4}\frac{\partial^2 A_{10}}{\partial \bar{y}^2} + \frac{1}{2}\bar{\eta}_1 A_{10} + \frac{1}{2}\zeta A_{10} \tag{57}$$

$$\begin{aligned} -\frac{\mathrm{i}}{2}A_{12} + \frac{1}{2}\frac{\partial A_{11}}{\partial \bar{t}} - \frac{i}{2}\bar{\eta}_1 A_{10} + \frac{\mathrm{i}}{4}B_{20}A_{10}^* - \mathrm{i}A_{20}B_{10}^* - \frac{\mathrm{i}}{2}\zeta A_{10} \\ +\frac{\mathrm{i}}{16}B_{10}^2 A_{10}^* - \frac{\mathrm{i}}{8}|B_{10}|^2 A_{10} + A_{20}A_{10}^* + \frac{\mathrm{i}}{2}UA_{11} \\ +\frac{1}{2}U\frac{\partial A_{10}}{\partial \bar{x}} + \frac{1}{2}V\frac{\partial A_{10}}{\partial \bar{y}} + \frac{1}{2}|A_{10}|^2 B_{10} + \frac{1}{2}B_{12} = 0 \end{aligned} \tag{58}$$

Using the results from first and second order (42, 44, 47–48, 51–52) gives the current modified cubic nonlinear Schrödinger equation:

$$\begin{aligned} \frac{\partial A_{11}}{\partial \bar{x}} + 2\frac{\partial A_{11}}{\partial \bar{t}} + 2\mathrm{i}UA_{11} + \mathrm{i}\frac{\partial^2 A_{10}}{\partial \bar{t}^2} - 6U\frac{\partial A_{10}}{\partial \bar{t}} \\ +\mathrm{i}|A_{10}|^2 A_{10} - 5\mathrm{i}U^2 A_{10} + 2V\frac{\partial A_{10}}{\partial \bar{y}} - \frac{\mathrm{i}}{2}\frac{\partial^2 A_{10}}{\partial \bar{y}^2} = 0 \end{aligned} \tag{59}$$

and

$$\begin{aligned} B_{12} &= iA_{12} - \frac{\partial A_{11}}{\partial \bar{t}} + \mathrm{i}\zeta A_{10} - \frac{3\mathrm{i}}{8}|A_{10}|^2 A_{10} - \mathrm{i}UA_{11} \\ &\quad +2U\frac{\partial A_{10}}{\partial \bar{t}} + 2\mathrm{i}U^2 A_{10} - V\frac{\partial A_{10}}{\partial \bar{y}} \end{aligned} \tag{60}$$

The second harmonic terms of third order of ϵ in the surface equations (40–41) are:

$$\begin{aligned} -\mathrm{i}B_{21} + \frac{1}{2}\frac{\partial B_{20}}{\partial \bar{t}} - \frac{1}{2}A_{10}B_{11} + \frac{\mathrm{i}}{4}A_{10}\frac{\partial B_{10}}{\partial \bar{x}} - \frac{1}{2}B_{10}A_{11} + \frac{3i}{4}\frac{\partial A_{10}}{\partial \bar{x}}B_{10} \\ +\mathrm{i}UB_{20} = A_{21} - \frac{\mathrm{i}}{2}\frac{\partial A_{20}}{\partial \bar{x}} \end{aligned} \tag{61}$$

$$\begin{aligned} -\mathrm{i}A_{21} + \frac{1}{2}\frac{\partial A_{20}}{\partial \bar{t}} - \frac{\mathrm{i}}{4}B_{10}A_{11} - \frac{1}{4}B_{10}\frac{\partial A_{10}}{\partial \bar{x}} + \frac{1}{4}B_{10}\frac{\partial A_{10}}{\partial \bar{t}} - \frac{\mathrm{i}}{4}A_{10}B_{11} \\ +\mathrm{i}UA_{20} + \frac{\mathrm{i}}{4}UA_{10}B_{10} + \frac{1}{2}B_{21} = 0 \end{aligned} \tag{62}$$

Using the results from first and second order (42, 47–48, 51–52) gives:

$$A_{21} = 0 \tag{63}$$

$$B_{21} = -2\mathrm{i}A_{10}\frac{\partial A_{10}}{\partial \bar{t}} - A_{10}A_{11} + 2UA_{10}^2 \tag{64}$$

The third harmonic terms of third order of ϵ in the surface equations (40–41) are:

$$-\frac{3\mathrm{i}}{2}B_{30} - \frac{3}{4}A_{10}B_{20} - \frac{3}{2}A_{20}B_{10} - \frac{3}{16}B_{10}^2 A_{10} = \frac{3}{2}A_{30} \tag{65}$$

$$-\frac{3\mathrm{i}}{2}A_{30} - \mathrm{i}B_{10}A_{20} - \frac{\mathrm{i}}{4}B_{20}A_{10} - \frac{\mathrm{i}}{16}B_{10}^2 A_{10} + \frac{1}{2}B_{30} = 0 \tag{66}$$

Using the results from first and second order (42, 51–52) gives:

$$A_{30} = 0 \tag{67}$$

$$B_{30} = -\frac{3\mathrm{i}}{8}A_{10}^3 \tag{68}$$

Fourth order The first harmonic terms of fourth order of ϵ in the surface equations (40–41) are:

$$\begin{aligned}
&-\frac{\mathrm{i}}{2}B_{13}+\frac{1}{2}\frac{\partial B_{12}}{\partial \bar{t}}+\frac{\mathrm{i}}{2}\frac{\partial \bar{\phi}_1}{\partial \bar{x}}B_{10}+\frac{\mathrm{i}}{2}\frac{\partial \bar{\eta}_1}{\partial \bar{x}}A_{10}+\mathrm{i}\bar{\eta}_1\frac{\partial A_{10}}{\partial \bar{x}}-\frac{1}{2}\bar{\eta}_1 A_{11}-\frac{1}{2}\bar{\eta}_2 A_{10}\\
&\quad-\frac{1}{2}A_{20}B_{11}^*-\frac{1}{2}A_{21}B_{10}^*+\frac{1}{4}B_{20}A_{11}^*+\frac{1}{4}B_{21}A_{10}^*-\frac{1}{8}A_{10}B_{11}B_{10}^*\\
&\quad-\frac{1}{8}A_{10}B_{10}B_{11}^*+\frac{1}{8}B_{10}B_{11}A_{10}^*+\frac{1}{16}B_{10}^2A_{11}^*-\frac{1}{8}|B_{10}|^2A_{11}\\
&\quad+\frac{\mathrm{i}}{2}A_{20}\frac{\partial B_{10}^*}{\partial \bar{x}}+\frac{\mathrm{i}}{8}A_{10}B_{10}\frac{\partial B_{10}^*}{\partial \bar{x}}+\frac{\mathrm{i}}{16}B_{10}^2\frac{\partial A_{10}^*}{\partial \bar{x}}+\frac{3\mathrm{i}}{8}|B_{10}|^2\frac{\partial A_{10}}{\partial \bar{x}}\\
&\quad+\frac{3\mathrm{i}}{4}\frac{\partial A_{20}}{\partial \bar{x}}B_{10}^*-\frac{\mathrm{i}}{4}\frac{\partial B_{20}}{\partial \bar{x}}A_{10}^*+\frac{\mathrm{i}}{8}A_{10}\frac{\partial B_{10}}{\partial \bar{x}}B_{10}^*-\frac{\mathrm{i}}{8}B_{10}\frac{\partial B_{10}}{\partial \bar{x}}A_{10}^*\\
&\quad+\frac{i}{2}UB_{12}+\frac{1}{2}U\frac{\partial B_{11}}{\partial \bar{x}}+\frac{1}{2}V\frac{\partial B_{11}}{\partial \bar{y}}-\frac{1}{2}\zeta A_{11}+i\zeta\frac{\partial A_{10}}{\partial \bar{x}}\\
&\quad=\frac{1}{2}A_{13}-\frac{\mathrm{i}}{2}\frac{\partial A_{12}}{\partial \bar{x}}-\frac{1}{4}\frac{\partial^2 A_{11}}{\partial \bar{y}^2}-\frac{\mathrm{i}}{4}\frac{\partial^3 A_{10}}{\partial \bar{x}\partial \bar{y}^2}
\end{aligned} \tag{69}$$

$$\begin{aligned}
&-\frac{\mathrm{i}}{2}A_{13}+\frac{1}{2}B_{13}+\frac{1}{2}\frac{\partial A_{12}}{\partial \bar{t}}+\frac{\mathrm{i}}{2}\frac{\partial \bar{\phi}_1}{\partial \bar{x}}A_{10}+\frac{1}{2}\frac{\partial \bar{\phi}_1}{\partial z}A_{10}-\frac{\mathrm{i}}{2}\bar{\eta}_1 A_{11}-\frac{1}{2}\bar{\eta}_1\frac{\partial A_{10}}{\partial \bar{x}}\\
&\quad+\frac{1}{2}\bar{\eta}_1\frac{\partial A_{10}}{\partial \bar{t}}-\frac{\mathrm{i}}{2}\bar{\eta}_2 A_{10}-\mathrm{i}A_{20}B_{11}^*+2A_{20}A_{11}^*+2A_{21}A_{10}^*-\mathrm{i}A_{21}B_{10}^*\\
&\quad+\frac{\mathrm{i}}{4}B_{20}A_{11}^*+\frac{\mathrm{i}}{4}B_{21}A_{10}^*+\frac{1}{2}A_{10}B_{11}A_{10}^*-\frac{\mathrm{i}}{8}A_{10}B_{11}B_{10}^*\\
&\quad+\frac{1}{2}A_{10}B_{10}A_{11}^*-\frac{\mathrm{i}}{8}A_{10}B_{10}B_{11}^*+\frac{1}{2}A_{11}B_{10}A_{10}^*-\frac{\mathrm{i}}{8}B_{10}A_{11}B_{10}^*\\
&\quad+\frac{\mathrm{i}}{8}B_{10}B_{11}A_{10}^*+\frac{\mathrm{i}}{16}B_{10}^2A_{11}^*+2\mathrm{i}A_{20}\frac{\partial A_{10}^*}{\partial \bar{x}}-\frac{1}{4}B_{20}\frac{\partial A_{10}^*}{\partial \bar{x}}+\frac{1}{4}B_{20}\frac{\partial A_{10}^*}{\partial \bar{t}}\\
&\quad+\frac{3\mathrm{i}}{4}A_{10}B_{10}\frac{\partial A_{10}^*}{\partial \bar{x}}-\frac{1}{8}B_{10}^2\frac{\partial A_{10}^*}{\partial \bar{x}}+\frac{1}{16}B_{10}^2\frac{\partial A_{10}^*}{\partial \bar{t}}-i\frac{\partial A_{20}}{\partial \bar{x}}A_{10}^*\\
&\quad-\frac{1}{2}\frac{\partial A_{20}}{\partial \bar{x}}B_{10}^*+\frac{1}{2}\frac{\partial A_{20}}{\partial \bar{t}}B_{10}^*-\frac{3\mathrm{i}}{4}B_{10}\frac{\partial A_{10}}{\partial \bar{x}}A_{10}^*-\frac{1}{4}B_{10}\frac{\partial A_{10}}{\partial \bar{x}}B_{10}^*\\
&\quad+\frac{1}{8}B_{10}\frac{\partial A_{10}}{\partial \bar{t}}B_{10}^*+\frac{\mathrm{i}}{2}UA_{12}+\mathrm{i}UA_{20}B_{10}^*-\frac{\mathrm{i}}{4}UB_{20}A_{10}^*-\frac{\mathrm{i}}{16}UB_{10}^2A_{10}^*\\
&\quad+\frac{\mathrm{i}}{8}U|B_{10}|^2A_{10}+\frac{1}{2}U\frac{\partial A_{11}}{\partial \bar{x}}+\frac{1}{2}V\frac{\partial A_{11}}{\partial \bar{y}}+\frac{1}{2}U\frac{\partial U}{\partial z}B_{10}+\frac{1}{2}V\frac{\partial V}{\partial z}B_{10}
\end{aligned}$$

$$
\begin{aligned}
&-\frac{\mathrm{i}}{2}\zeta A_{11} - \frac{1}{2}\zeta\frac{\partial A_{10}}{\partial \overline{x}} + \frac{1}{2}\zeta\frac{\partial A_{10}}{\partial \overline{t}} + \frac{\mathrm{i}}{2}\zeta U A_{10} \\
&= 0
\end{aligned} \tag{70}
$$

Using the results from first, second and third order (42, 44, 47–48, 51–52, 55–56, 59–60, 63–64, 67–68) gives the current modified nonlinear Schrödinger equation built on potential theory to Dysthe level, MNLSC:

$$
\begin{aligned}
&\frac{\partial A_{12}}{\partial \overline{x}} + 2\frac{\partial A_{12}}{\partial \overline{t}} + \mathrm{i}\frac{\partial^2 A_{11}}{\partial \overline{t}^2} + 2\mathrm{i}\frac{\partial \overline{\phi}_1}{\partial \overline{x}}A_{10} - \frac{\mathrm{i}}{2}\frac{\partial^2 A_{11}}{\partial \overline{y}^2} - \frac{\partial^3 A_{10}}{\partial \overline{t}\partial \overline{y}^2} \\
&\quad -8A_{10}\frac{\partial A_{10}}{\partial \overline{t}}A_{10}^* + \mathrm{i}A_{10}^2 A_{11}^* + 2\mathrm{i}A_{10}A_{11}A_{10}^* + 2\mathrm{i}UA_{12} - 6U\frac{\partial A_{11}}{\partial \overline{t}} \\
&\quad -6\mathrm{i}U\frac{\partial^2 A_{10}}{\partial \overline{t}^2} - 10\mathrm{i}UA_{10}^2 A_{10}^* + 2V\frac{\partial A_{11}}{\partial \overline{y}} + 2\mathrm{i}V\frac{\partial^2 A_{10}}{\partial \overline{t}\partial \overline{y}} - 5\mathrm{i}U^2 A_{11} \\
&\quad +20U^2\frac{\partial A_{10}}{\partial \overline{t}} + \mathrm{i}U\frac{\partial U}{\partial z}A_{10} - 6UV\frac{\partial A_{10}}{\partial \overline{y}} + \mathrm{i}V\frac{\partial V}{\partial z}A_{10} + 14\mathrm{i}U^3 A_{10} \\
&\quad = 0
\end{aligned} \tag{71}
$$

3.1.3 Summary

In the following $A = A_1$, $B = B_1$, and $(\bar{x}, \bar{y}, \bar{t}) = (x, y, t)$ to simplify the notation.

Space evolution of A The space evolution of the MNLSC equation (71) expressed by modulation of A is:

$$
\begin{aligned}
&\frac{\partial A}{\partial x} + 2\frac{\partial A}{\partial t} + 2iUA \\
&\quad +\mathrm{i}\frac{\partial^2 A}{\partial t^2} - \frac{\mathrm{i}}{2}\frac{\partial^2 A}{\partial y^2} + \mathrm{i}A|A|^2 - 6U\frac{\partial A}{\partial t} - 5\mathrm{i}U^2 A + 2V\frac{\partial A}{\partial y} \\
&\quad +2\mathrm{i}\frac{\partial \overline{\phi}}{\partial x}A - \frac{\partial^3 A}{\partial t\partial y^2} - 8|A|^2\frac{\partial A}{\partial t} - 6\mathrm{i}U\frac{\partial^2 A}{\partial t^2} - 10\mathrm{i}UA|A|^2 + 2iV\frac{\partial^2 A}{\partial t\partial y} \\
&\quad +20U^2\frac{\partial A}{\partial t} + \mathrm{i}U\frac{\partial U}{\partial z}A - 6UV\frac{\partial A}{\partial y} + \mathrm{i}V\frac{\partial V}{\partial z}A + 14\mathrm{i}U^3 A = 0
\end{aligned} \tag{72}
$$

and

$$
\frac{\partial \overline{\phi}}{\partial z} = -\frac{\partial |A|^2}{\partial t} \qquad \text{when } z = 0 \tag{73}
$$

$$
4\frac{\partial^2 \overline{\phi}}{\partial t^2} + \frac{\partial^2 \overline{\phi}}{\partial y^2} + \frac{\partial^2 \overline{\phi}}{\partial z^2} = 0 \qquad \text{when } z < 0 \tag{74}
$$

$$
\frac{\partial \overline{\phi}}{\partial z} = 0 \qquad \text{when } z \to -\infty \tag{75}
$$

with the following reconstruction formulas:

$$\begin{aligned}
\overline{\eta} &= -\frac{\partial\overline{\phi}}{\partial t} \\
A_2, A_3 &= 0 \\
B &= \mathrm{i}A - \frac{\partial A}{\partial t} - \mathrm{i}UA + \mathrm{i}\zeta A - \frac{3\mathrm{i}}{8}A|A|^2 + 2U\frac{\partial A}{\partial t} + 2\mathrm{i}U^2 A - V\frac{\partial A}{\partial y} \\
B_2 &= -\frac{1}{2}A^2 - 2\mathrm{i}A\frac{\partial A}{\partial t} + 2UA^2 \\
B_3 &= -\frac{3i}{8}A^3
\end{aligned}$$

Space evolution of B The space evolution of the MNLSC equation (71) expressed by modulation of B is:

$$\begin{aligned}
&\frac{\partial B}{\partial x} + 2\frac{\partial B}{\partial t} + 2\mathrm{i}UB \\
&\quad +\mathrm{i}\frac{\partial^2 B}{\partial t^2} - \frac{\mathrm{i}}{2}\frac{\partial^2 B}{\partial y^2} + \mathrm{i}B|B|^2 - 6U\frac{\partial B}{\partial t} - 5\mathrm{i}U^2 B + 2V\frac{\partial B}{\partial y} - 4\mathrm{i}\frac{\partial\overline{\phi}_1}{\partial t}B \\
&\quad -\frac{\partial^3 B}{\partial t\partial y^2} - 8|B|^2\frac{\partial B}{\partial t} - 2B^2\frac{\partial B^*}{\partial t} - 6\mathrm{i}U\frac{\partial^2 B}{\partial t^2} - 8\mathrm{i}U|B|^2 B + 2\mathrm{i}V\frac{\partial^2 B}{\partial t\partial y} \\
&\quad +20U^2\frac{\partial B}{\partial t} + \mathrm{i}U\frac{\partial U}{\partial z}B - 6UV\frac{\partial B}{\partial y} + \mathrm{i}V\frac{\partial V}{\partial z}B + 14\mathrm{i}U^3 B = 0 \qquad (76)
\end{aligned}$$

and

$$\begin{aligned}
\frac{\partial\overline{\phi}}{\partial z} &= -\frac{\partial|B|^2}{\partial t} \qquad \text{when } z = 0 \qquad (77) \\
\frac{\partial^2\overline{\phi}}{\partial x^2} + \frac{\partial^2\overline{\phi}}{\partial y^2} + \frac{\partial^2\overline{\phi}}{\partial z^2} &= 0 \qquad \text{when } z < 0 \qquad (78) \\
\frac{\partial\overline{\phi}}{\partial z} &= 0 \qquad \text{when } z \to -\infty \qquad (79)
\end{aligned}$$

with the following reconstruction formulas:

$$\begin{aligned}
\overline{\eta} &= -\frac{\partial\overline{\phi}}{\partial t} \\
A &= -\mathrm{i}B - \frac{\partial B}{\partial t} - \mathrm{i}UB + \mathrm{i}\frac{\partial^2 B}{\partial t^2} + \mathrm{i}\zeta B - \frac{3\mathrm{i}}{8}|B|^2 B + \mathrm{i}U^2 B - V\frac{\partial B}{\partial y} \\
A_2, A_3 &= 0 \\
B_2 &= \frac{1}{2}B^2 + \mathrm{i}B\frac{\partial B}{\partial t} - UB^2 \\
B_3 &= \frac{3}{8}B^3
\end{aligned}$$

Time evolution of A The time evolution of the MNLSC equation (71) expressed by modulation of A is:

$$\begin{aligned}
&\frac{\partial A}{\partial t}+\frac{1}{2}\frac{\partial A}{\partial x}+\mathrm{i}UA\\
&\quad+\frac{\mathrm{i}}{8}\frac{\partial^2 A}{\partial x^2}-\frac{\mathrm{i}}{4}\frac{\partial^2 A}{\partial y^2}+\frac{\mathrm{i}}{2}A|A|^2+U\frac{\partial A}{\partial x}+V\frac{\partial A}{\partial y}\\
&\quad+\mathrm{i}\frac{\partial\overline{\phi}}{\partial x}A-\frac{1}{16}\frac{\partial^3 A}{\partial x^3}+\frac{3}{8}\frac{\partial^3 A}{\partial x\partial y^2}+\frac{3}{2}|A|^2\frac{\partial A}{\partial x}-\frac{1}{4}A^2\frac{\partial A^*}{\partial x}\\
&\quad+\frac{\mathrm{i}}{2}U\frac{\partial U}{\partial z}A+\frac{\mathrm{i}}{2}V\frac{\partial V}{\partial z}A=0
\end{aligned}\tag{80}$$

and

$$\frac{\partial\overline{\phi}}{\partial z} = \frac{1}{2}\frac{\partial|A|^2}{\partial x} \qquad \text{when } z=0 \tag{81}$$

$$\frac{\partial^2\overline{\phi}}{\partial x^2}+\frac{\partial^2\overline{\phi}}{\partial y^2}+\frac{\partial^2\overline{\phi}}{\partial z^2} = 0 \qquad \text{when } z<0 \tag{82}$$

$$\frac{\partial\overline{\phi}}{\partial z} = 0 \qquad \text{when } z\to-\infty \tag{83}$$

with the following reconstruction formulas:

$$\begin{aligned}
\overline{\eta} &= \frac{1}{2}\frac{\partial\overline{\phi}}{\partial x}\\
A_2, A_3 &= 0\\
B &= \mathrm{i}A+\frac{1}{2}\frac{\partial A}{\partial x}+\mathrm{i}\zeta A+\frac{\mathrm{i}}{8}A|A|^2+\frac{\mathrm{i}}{8}\frac{\partial^2 A}{\partial x^2}-\frac{\mathrm{i}}{4}\frac{\partial^2 A}{\partial y^2}\\
B_2 &= -\frac{1}{2}A^2+\mathrm{i}A\frac{\partial A}{\partial x}\\
B_3 &= -\frac{3\mathrm{i}}{8}A^3
\end{aligned}$$

Time evolution of B The time evolution of the MNLSC equation (71) expressed by modulation of B is:

$$\begin{aligned}
&\frac{\partial B}{\partial t}+\frac{1}{2}\frac{\partial B}{\partial x}+\mathrm{i}UB\\
&\quad+\frac{\mathrm{i}}{8}\frac{\partial^2 B}{\partial x^2}-\frac{\mathrm{i}}{4}\frac{\partial^2 B}{\partial y^2}+\frac{\mathrm{i}}{2}|B|^2B+U\frac{\partial B}{\partial x}+V\frac{\partial B}{\partial y}\\
&\quad-\frac{1}{16}\frac{\partial^3 B}{\partial x^3}+\frac{3}{8}\frac{\partial^3 B}{\partial x\partial y^2}+\frac{3}{2}B\frac{\partial B}{\partial x}B^*+\frac{1}{4}B^2\frac{\partial B^*}{\partial x}+i\frac{\partial\overline{\phi}_1}{\partial x}B\\
&\quad+\frac{\mathrm{i}}{2}U\frac{\partial U}{\partial z}B+\frac{\mathrm{i}}{2}V\frac{\partial V}{\partial z}B-\frac{\mathrm{i}}{2}U|B|^2B=0
\end{aligned}\tag{84}$$

and

$$\frac{\partial\overline{\phi}}{\partial z} = \frac{1}{2}\frac{\partial|B|^2}{\partial x} \qquad \text{when } z=0 \tag{85}$$

$$\frac{\partial^2\overline{\phi}}{\partial x^2}+\frac{\partial^2\overline{\phi}}{\partial y^2}+\frac{\partial^2\overline{\phi}}{\partial z^2} = 0 \qquad \text{when } z<0 \tag{86}$$

$$\frac{\partial\overline{\phi}}{\partial z} = 0 \qquad \text{when } z\to-\infty \tag{87}$$

with the following reconstruction formulas:

$$\begin{aligned}
\overline{\eta} &= \frac{1}{2}\frac{\partial\overline{\phi}}{\partial x}\\
A &= -\mathrm{i}B+\frac{1}{2}\frac{\partial B}{\partial x}+\frac{3\mathrm{i}}{8}\frac{\partial^2 B}{\partial x^2}-\frac{\mathrm{i}}{4}\frac{\partial^2 B}{\partial y^2}+\frac{\mathrm{i}}{8}|B|^2B+\mathrm{i}\zeta B\\
A_2, A_3 &= 0\\
B_2 &= \frac{1}{2}B^2-\frac{\mathrm{i}}{2}B\frac{\partial B}{\partial x}\\
B_3 &= \frac{3}{8}B^3
\end{aligned}$$

The CNLS^4 equation by Stocker & Peregrine (1999) may be derived from (84) by rescaling.

3.2 Current field with horizontal shear

If the current field is rotational, vorticity develops in the wave field according to (19).

The divergence of the Euler equation for the waves (18) is:

$$\nabla\cdot(\boldsymbol{v}\cdot\nabla\boldsymbol{v}+\boldsymbol{v}\cdot\nabla\boldsymbol{V}+\boldsymbol{V}\cdot\nabla\boldsymbol{v}) = -\frac{1}{\rho}\nabla^2 p \tag{88}$$

The surface equations for the combined field at $z=\eta+\zeta$ can be written as:

$$\frac{\partial\eta}{\partial t}+\boldsymbol{v}_{tot}\cdot\boldsymbol{\nabla}(\eta+\zeta) = w+W \tag{89}$$

$$p_{tot} = p \tag{90}$$

Taylor expansions around $z=0$ gives (89–90) on the form:

$$\frac{\partial\eta}{\partial t}+\boldsymbol{v}_{tot}\cdot\boldsymbol{\nabla}(\eta+\zeta)+(\eta+\zeta)\frac{\partial\boldsymbol{v}_{tot}}{\partial z}\cdot\boldsymbol{\nabla}(\eta+\zeta)+\frac{1}{2}(\eta+\zeta)^2\frac{\partial^2\boldsymbol{v}_{tot}}{\partial z^2}\cdot\boldsymbol{\nabla}(\eta+\zeta)$$

$$= w + W + (\eta+\zeta)\frac{\partial}{\partial z}(w+W) + \frac{1}{2}(\eta+\zeta)\frac{\partial^2}{\partial z^2}(w+W) + \cdots \tag{91}$$

$$p_{tot} + (\eta+\zeta)\frac{\partial p_{tot}}{\partial z} + \frac{1}{2}(\eta+\zeta)^2\frac{\partial^2 p_{tot}}{\partial z^2} + \cdots = p_a \tag{92}$$

The waves are assumed on deep water, thus $\boldsymbol{v}, p \to 0$ as $z \to -\infty$.

Let the current vary more slowly on a length scale along the x–axis, X, than along the y–axis, Y, so that $1/(k_c X) = O(\epsilon)$ and $1/(k_c Y) = O(1)$. In accordance with the scaling assumptions, all equations, variables, and sizes in the following are made dimensionless using the characteristic length and time scales of the wave field, so that $k_c\boldsymbol{x} \to \boldsymbol{x}$, $\epsilon k_c \boldsymbol{x} \to \bar{\boldsymbol{x}}$, $\omega_c t \to t$, $k_c\eta \to \epsilon\eta$, $k_c\zeta \to \epsilon^2\zeta$, $\frac{k_c}{\omega_c}\boldsymbol{v} \to \epsilon\boldsymbol{v}$, $\frac{k_c}{\omega_c}(U,V) \to \epsilon(U,V)$, $\frac{k_c}{\omega_c}W \to \epsilon^4 W$, $\frac{k_c}{\rho g}p \to \epsilon p$, and $\frac{k_c}{\rho g}P \to \epsilon^3 P$.

Note that in Hjelmervik & Trulsen (2009) the scaling is slightly changed. Since the waves are modulated on a length scale of order ϵ, the transversal length scale of the current is also assumed of order ϵ. And the vertical surface velocity of the current is assumed of one order lower.

The scaled equation for the divergence of the Euler equation for the waves (88) to the fourth order of ϵ is:

$$\begin{aligned}\epsilon\left(\left(\frac{\partial u}{\partial x}\right)^2+\left(\frac{\partial v}{\partial u}\right)^2+\left(\frac{\partial w}{\partial z}\right)^2+2\frac{\partial u}{\partial y}\frac{\partial v}{\partial x}+2\frac{\partial u}{\partial z}\frac{\partial w}{\partial x}+2\frac{\partial v}{\partial z}\frac{\partial w}{\partial y}+2\frac{\partial v}{\partial x}\frac{\partial U}{\partial y}+2\frac{\partial v}{\partial y}\frac{\partial V}{\partial y}\right)\\ +\epsilon^2\left(2\frac{\partial u}{\partial x}\frac{\partial U}{\partial x}+2\frac{\partial u}{\partial y}\frac{\partial V}{\partial x}\right) = -\frac{\partial^2 p}{\partial x^2}-\frac{\partial^2 p}{\partial y^2}-\frac{\partial^2 p}{\partial z^2}\end{aligned} \tag{93}$$

The scaled Euler equation for the waves (18) to the fourth order of ϵ is:

$$\frac{\partial u}{\partial t} + \epsilon\left(U\frac{\partial u}{\partial x} + V\frac{\partial u}{\partial y} + v\frac{\partial U}{\partial y} + \boldsymbol{v}\cdot\boldsymbol{\nabla}u\right) + \epsilon^2 u\frac{\partial U}{\partial x} = -\frac{\partial p}{\partial x} \tag{94}$$

$$\frac{\partial v}{\partial t} + \epsilon\left(U\frac{\partial v}{\partial x} + V\frac{\partial v}{\partial y} + v\frac{\partial V}{\partial y} + \boldsymbol{v}\cdot\boldsymbol{\nabla}v\right) + \epsilon^2 u\frac{\partial V}{\partial x} = -\frac{\partial p}{\partial y} \tag{95}$$

$$\frac{\partial w}{\partial t} + \epsilon\left(U\frac{\partial w}{\partial x} + V\frac{\partial w}{\partial y} + \boldsymbol{v}\cdot\boldsymbol{\nabla}w\right) = -\frac{\partial p}{\partial z} \tag{96}$$

The scaled surface equations for the waves (91–92) to the fourth order of ϵ is:

$$\begin{aligned}\frac{\partial \eta}{\partial t} + \epsilon(\boldsymbol{v}+\boldsymbol{V})\cdot\boldsymbol{\nabla}\eta + \epsilon^2\left(v\frac{\partial\zeta}{\partial y} + \eta\frac{\partial \boldsymbol{v}}{\partial z}\cdot\boldsymbol{\nabla}\eta\right)\\ +\epsilon^3\left(u\frac{\partial\zeta}{\partial x} + \eta\frac{\partial v}{\partial z}\frac{\partial\zeta}{\partial y} + \zeta\frac{\partial\boldsymbol{v}}{\partial z}\cdot\boldsymbol{\nabla}\eta + \frac{1}{2}\eta^2\frac{\partial^2\boldsymbol{v}}{\partial z^2}\cdot\boldsymbol{\nabla}\eta\right)\end{aligned}$$

$$= w + \epsilon\eta\frac{\partial w}{\partial z} + \epsilon^2\left(\zeta\frac{\partial w}{\partial z} + \frac{1}{2}\eta^2\frac{\partial^2 w}{\partial z^2}\right) + \epsilon^3\left(\eta\zeta\frac{\partial^2 w}{\partial z^2} + \frac{1}{6}\eta^3\frac{\partial^3 w}{\partial z^3}\right) + O(\epsilon^4) \quad (97)$$

$$p - \eta + \epsilon\eta\frac{\partial p}{\partial z} + \epsilon^2\left(\zeta\frac{\partial p}{\partial z} + \frac{1}{2}\eta^2\frac{\partial^2 p}{\partial z^2}\right) + \epsilon^3\left(\eta\zeta\frac{\partial^2 p}{\partial z^2} + \frac{1}{6}\eta^3\frac{\partial^3 p}{\partial z^3}\right) = O(\epsilon^4) \quad (98)$$

The wave field is represented by perturbation series for the surface displacement, η, the velocity, $\boldsymbol{v}$, and the dynamic pressure, p:

$$\begin{aligned}
\eta &= \epsilon\bar{\eta} + \tfrac{1}{2}\Big(B_1\mathrm{e}^{\mathrm{i}(x-t)} + \epsilon B_2\mathrm{e}^{2\mathrm{i}(x-t)} + \epsilon^2 B_3\mathrm{e}^{3\mathrm{i}(x-t)} + \cdots + \text{c.c.}\Big)\\
\boldsymbol{v} &= \epsilon\bar{\boldsymbol{v}} + \tfrac{1}{2}\Big(\boldsymbol{v}_1\mathrm{e}^{\mathrm{i}(x-t)} + \epsilon\boldsymbol{v}_2\mathrm{e}^{2\mathrm{i}(x-t)} + \epsilon^2\boldsymbol{v}_3\mathrm{e}^{3\mathrm{i}(x-t)} + \cdots + \text{c.c.}\Big)\\
p &= \epsilon\bar{p} + \tfrac{1}{2}\Big(p_1\mathrm{e}^{\mathrm{i}(x-t)} + \epsilon p_2\mathrm{e}^{2\mathrm{i}(x-t)} + \epsilon^2 p_3\mathrm{e}^{3\mathrm{i}(x-t)} + \cdots + \text{c.c.}\Big)
\end{aligned} \quad (99)$$

We shall assume that the waves are modulated on the slow spatial scales $\bar{x}$ and $\bar{y}$, and a correspondingly slow time scale $\epsilon t = \bar{t}$. Thus $\bar{\eta} = \bar{\eta}(\bar{x},\bar{y},\bar{t})$, $\boldsymbol{v} = \bar{\boldsymbol{v}}(\bar{x},\bar{y},z,\bar{t})$, and $\boldsymbol{p} = \bar{p}(\bar{x},\bar{y},z,\bar{t})$ are the mean surface displacement, mean induced velocity, and mean dynamic pressure respectively, while $B_n = B_n(\bar{x},\bar{y},\bar{t})$, $\boldsymbol{v}_n = \boldsymbol{v}_n(\bar{x},\bar{y},z,\bar{t})$, and $p_n = p_n(\bar{x},\bar{y},z,\bar{t})$ are the n'th harmonics of the surface displacement, induced current, and dynamic pressure respectively. The characteristic wavenumber is fixed appropriate for waves undisturbed by current, therefore the entire effect of refraction is represented by the modulation of B_1.

Both the mean functions and the harmonics, are perturbed:

$$\begin{aligned}
\bar{\eta} &= \bar{\eta}_1 + \epsilon\bar{\eta}_2 + \cdots, & B_n &= B_{n0} + \epsilon B_{n1} + \epsilon^2 B_{n2} + \cdots\\
\bar{\boldsymbol{v}} &= \bar{\boldsymbol{v}}_1 + \epsilon\bar{\boldsymbol{v}}_2 + \cdots, & \boldsymbol{v}_n &= \boldsymbol{v}_{n0} + \epsilon\boldsymbol{v}_{n1} + \epsilon^2\boldsymbol{v}_{n2} + \cdots\\
\bar{p} &= \bar{p}_1 + \epsilon\bar{p}_2 + \cdots, & p_n &= p_{n0} + \epsilon p_{n1} + \epsilon^2 p_{n2} + \cdots
\end{aligned} \quad (100)$$

3.2.1 First order terms

First harmonic The first harmonic terms of first order of ϵ for the divergence of the Euler equation (93) are:

$$p_{10} - \frac{\partial^2 p_{10}}{\partial z^2} = 0 \quad (101)$$

which has the general solution:

$$p_{10} = A_{10}(\bar{x},\bar{y},\bar{t})\mathrm{e}^z \quad (102)$$

The first harmonic terms of first order of ϵ in the surface equations (97–98) give:

$$A_{10} = B_{10} \quad (103)$$

The first harmonic terms of first order of ϵ in the Euler equation (94–96) then give respectively:

$$u_{10} = B_{10}\mathrm{e}^z \tag{104}$$
$$v_{10} = 0 \tag{105}$$
$$w_{10} = -\mathrm{i}B_{10}\mathrm{e}^z \tag{106}$$

3.2.2 Second order terms

Zeroth harmonic The zeroth harmonic terms of second order of ϵ for the z–component of the Euler equation (96) are:

$$\frac{\mathrm{i}}{4}u_{10}w_{10}^* + \frac{\mathrm{i}}{4}u_{10}^*w_{10} + \frac{1}{4}w_{10}\frac{\partial w_{10}^*}{\partial z} + \frac{1}{4}w_{10}^*\frac{\partial w_{10}}{\partial z} = -\frac{\partial \bar{p}_1}{\partial z} \tag{107}$$

Using the results from first order (104, 106) gives:

$$|B_{10}|^2\mathrm{e}^{2z} = -\frac{\partial \bar{p}_1}{\partial z} \tag{108}$$

which has the solution:

$$\bar{p}_1 = \bar{A}_1(\bar{x},\bar{y},\bar{t})\mathrm{e}^z - \frac{1}{2}|B_{10}|^2\mathrm{e}^{2z} \tag{109}$$

The zeroth harmonic terms of second order of ϵ in the dynamic surface equation (98) are:

$$\bar{p}_1\Big|_{z=0} - \bar{\eta}_1 + \frac{1}{4}B_{10}\frac{\partial p_{10}^*}{\partial z}\Big|_{z=0} + \frac{1}{4}B_{10}^*\frac{\partial p_{10}}{\partial z}\Big|_{z=0} = 0 \tag{110}$$

Using the results from first order (102–103) and the solution for $\bar{p}_1$ (109) gives $\bar{A}_1 = \bar{\eta}_1$.

The zeroth harmonic terms of second order of ϵ in the kinematic surface equation (97) are:

$$\begin{aligned} -\frac{\mathrm{i}}{4}u_{10}\Big|_{z=0}B_{10}^* + \frac{\mathrm{i}}{4}u_{10}^*\Big|_{z=0}B_{10} \\ = \bar{w}_1\Big|_{z=0} + \frac{1}{4}B_{10}\frac{\partial w_{10}^*}{\partial z}\Big|_{z=0} + \frac{1}{4}B_{10}^*\frac{\partial w_{10}}{\partial z}\Big|_{z=0} \end{aligned} \tag{111}$$

Using the results from first order (104, 106) gives:

$$\bar{w}_1\Big|_{z=0} = 0 \tag{112}$$

Since no surface elevation or induced current is provoked to first order of ϵ, $\bar{\eta}_1 = \bar{u}_1 = \bar{v}_1 = \bar{w}_1 = 0$ without lack of information.

First harmonic The first harmonic terms of second order of ϵ for the divergence of the Euler equation (93) are:

$$2\mathrm{i}v_{10}\frac{\partial U}{\partial y} + 2\mathrm{i}\frac{\partial p_{10}}{\partial \bar{x}} = p_{11} - \frac{\partial^2 p_{11}}{\partial z^2} \tag{113}$$

Using the results from first order (102–103, 105) gives:

$$2\mathrm{i}\frac{\partial B_{10}}{\partial \bar{x}}\mathrm{e}^z = p_{11} - \frac{\partial^2 p_{11}}{\partial z^2} \tag{114}$$

which has the solution:

$$p_{11} = A_{11}(\bar{x},\bar{y},\bar{t})\mathrm{e}^z - \mathrm{i}\frac{\partial B_{10}}{\partial \bar{x}} z\mathrm{e}^z \tag{115}$$

The first harmonic terms of second order of ϵ in the dynamic surface equation (98) give:

$$A_{11} = B_{11} \tag{116}$$

The first harmonic terms of second order of ϵ in the Euler equation and the kinematic surface equation (94–97) are respectively:

$$\frac{\partial u_{10}}{\partial \bar{t}} - \mathrm{i}u_{11} + \mathrm{i}u_{10}U + v_{10}\frac{\partial U}{\partial \bar{y}} = -\frac{\partial p_{10}}{\partial \bar{x}} - \mathrm{i}p_{11} \tag{117}$$

$$\frac{\partial v_{10}}{\partial \bar{t}} - \mathrm{i}v_{11} + \mathrm{i}v_{10}U + v_{10}\frac{\partial V}{\partial \bar{y}} = -\frac{\partial p_{10}}{\partial \bar{y}} \tag{118}$$

$$\frac{\partial w_{10}}{\partial \bar{t}} - \mathrm{i}w_{11} + \mathrm{i}w_{10}U = -\frac{\partial p_{11}}{\partial \bar{z}} \tag{119}$$

$$\frac{\partial B_{10}}{\partial \bar{t}} - \mathrm{i}B_{11} + \mathrm{i}UB_{10} = w_{11}\Big|_{z=0} \tag{120}$$

Using the results from first order (102–106) and the solution for p_{11} (115), leads to the current modified Schrödinger equation to linear order:

$$\frac{\partial B_{10}}{\partial \bar{x}} + 2\frac{\partial B_{10}}{\partial \bar{t}} + 2\mathrm{i}UB_{10} = 0 \tag{121}$$

and the following reconstruction formulas:

$$u_{11} = B_{11}\mathrm{e}^z + \mathrm{i}\left(\frac{\partial B_{10}}{\partial \bar{t}} + \mathrm{i}UB_{10}\right)(1+2z)\mathrm{e}^z \tag{122}$$

$$v_{11} = -\mathrm{i}\frac{\partial B_{10}}{\partial \bar{y}}\mathrm{e}^z \tag{123}$$

$$w_{11} = -\mathrm{i}B_{11}\mathrm{e}^z + \left(\frac{\partial B_{10}}{\partial \bar{t}} + \mathrm{i}UB_{10}\right)(1+2z)\mathrm{e}^z \tag{124}$$

Second harmonic The second harmonic terms of second order of ϵ for the divergence of the Euler equation (93) are:

$$-\frac{1}{2}u_{10}^2 + \frac{1}{2}\left(\frac{\partial w_{10}}{\partial z}\right)^2 + \mathrm{i}\frac{\partial u_{10}}{\partial z}w_{10} = 4p_{20} - \frac{\partial^2 p_{20}}{\partial z^2} \tag{125}$$

Using the results from first order (104, 106) gives:

$$0 = 4p_{20} - \frac{\partial^2 p_{20}}{\partial z^2} \tag{126}$$

which has the solution:

$$p_{20} = A_{20}\mathrm{e}^{2z} \tag{127}$$

The second harmonic terms of second order of ϵ in the dynamic surface equation (98) are:

$$p_{20}\big|_{z=0} - B_{20} + \frac{1}{2}B_{10}\frac{\partial p_{10}}{\partial z}\big|_{z=0} = 0 \tag{128}$$

Using the results from first order (102–103) and the solution for p_{20} (127) gives:

$$A_{20} = B_{20} - \frac{1}{2}B_{10}^2 \tag{129}$$

The second harmonic terms of second order of ϵ in the Euler equation and the kinematic surface equation (94–97) are respectively:

$$-\mathrm{i}u_{20} + \frac{\mathrm{i}}{4}u_{10}^2 + \frac{1}{4}w_{10}\frac{\partial u_{10}}{\partial z} = -ip_{20} \tag{130}$$

$$-\mathrm{i}v_{20} + \frac{\mathrm{i}}{4}u_{10}v_{10} + \frac{1}{4}w_{10}\frac{\partial v_{10}}{\partial z} = 0 \tag{131}$$

$$-\mathrm{i}w_{20} + \frac{\mathrm{i}}{4}u_{10}w_{10} + \frac{1}{4}w_{10}\frac{\partial w_{10}}{\partial z} = -\frac{1}{2}\frac{\partial p_{20}}{\partial z} \tag{132}$$

$$-\mathrm{i}B_{20} + \frac{\mathrm{i}}{4}u_{10}\big|_{z=0}B_{10} = \frac{1}{2}w_{20}\big|_{z=0} + \frac{1}{4}B_{10}\frac{\partial w_{10}}{\partial z}\big|_{z=0} \tag{133}$$

Using the results from first order (104–106) and the solution for p_{20} (127–129) gives:

$$u_{20} = v_{20} = w_{20} = p_{20} = 0 \tag{134}$$

$$B_{20} = \frac{1}{2}B_{10}^2 \tag{135}$$

3.2.3 Third order terms

First harmonic The first harmonic terms of third order of ϵ for the divergence of the Euler equation (93) are:

$$\begin{aligned} u_{20}u_{10}^* + \frac{1}{2}\frac{\partial w_{20}}{\partial z}\frac{\partial w_{10}^*}{\partial z} - \frac{\mathrm{i}}{2}\frac{\partial u_{20}}{\partial z}w_{10}^* + \mathrm{i}\frac{\partial u_{10}^*}{\partial z}w_{20} \\ +\mathrm{i}v_{11}\frac{\partial U}{\partial y} + \frac{\partial v_{10}}{\partial \bar{x}}\frac{\partial U}{\partial y} + \frac{\partial v_{10}}{\partial \bar{x}}\frac{\partial V}{\partial y} + \mathrm{i}u_{10}\frac{\partial U}{\partial x} \\ = -\frac{1}{2}\frac{\partial^2 p_{10}}{\partial \bar{x}^2} - \mathrm{i}\frac{\partial p_{11}}{\partial \bar{x}} + \frac{1}{2}p_{12} - \frac{1}{2}\frac{\partial^2 p_{10}}{\partial \bar{y}^2} - \frac{1}{2}\frac{\partial^2 p_{12}}{\partial z^2} \end{aligned} \quad (136)$$

Using the results from first and second order (102–106, 115–116, 123, 134) gives:

$$\begin{aligned} \frac{\partial^2 p_{12}}{\partial z^2} - p_{12} &= -2\mathrm{i}\frac{\partial B_{11}}{\partial \bar{x}}\mathrm{e}^z - \frac{\partial^2 B_{10}}{\partial \bar{x}^2}\mathrm{e}^z - \frac{\partial^2 B_{10}}{\partial \bar{y}^2}\mathrm{e}^z \\ &\quad -2\frac{\partial^2 B_{10}}{\partial \bar{x}^2}z\mathrm{e}^z - 2\mathrm{i}B_{10}\frac{\partial U}{\partial x}\mathrm{e}^z - 2\frac{\partial B_{10}}{\partial \bar{y}}\frac{\partial U}{\partial y}\mathrm{e}^z \end{aligned} \quad (137)$$

which has the solution:

$$p_{12} = A_{12}(\bar{x},\bar{y},\bar{z},\bar{t})\mathrm{e}^z + \alpha(\bar{x},\bar{y},\bar{z},\bar{t})z\mathrm{e}^z + \beta(\bar{x},\bar{y},\bar{t})z^2\mathrm{e}^z \quad (138)$$

where

$$\begin{aligned} \alpha &= -\mathrm{i}\frac{\partial B_{11}}{\partial \bar{x}} - \frac{1}{2}\frac{\partial^2 B_{10}}{\partial \bar{y}^2} - \mathrm{i}B_{10}\frac{\partial U}{\partial x} - \frac{\partial B_{10}}{\partial \bar{y}}\frac{\partial U}{\partial y} \\ \beta &= -\frac{1}{2}\frac{\partial^2 B_{10}}{\partial \bar{x}^2} \end{aligned}$$

The first harmonic terms of third order of ϵ in the dynamic surface equation (98) are:

$$\begin{aligned} \frac{1}{2}p_{12}\Big|_{z=0} - \frac{1}{2}B_{12} + \frac{1}{4}B_{20}\frac{\partial p_{10}^*}{\partial z}\Big|_{z=0} + \frac{1}{4}B_{10}^*\frac{\partial p_{20}}{\partial z}\Big|_{z=0} + \frac{1}{2}B_{10}\frac{\partial \bar{p}_1}{\partial z}\Big|_{z=0} \\ +\frac{1}{2}\zeta\frac{\partial p_{10}}{\partial z}\Big|_{z=0} + \frac{1}{16}B_{10}^2\frac{\partial^2 p_{10}^*}{\partial z^2}\Big|_{z=0} + \frac{1}{8}|B_{10}|^2\frac{\partial^2 p_{10}}{\partial z^2}\Big|_{z=0} &= 0 \end{aligned} \quad (139)$$

Using the results from the first and second order (102–103, 109, 134–135) and the solution for p_{12} (138), gives:

$$A_{12} = B_{12} + \frac{3}{8}B_{10}^2B_{10}^* - B_{10}\zeta \qquad \text{at } z = 0 \quad (140)$$

The first harmonic terms of third order of ϵ in the Euler equation and the kinematic surface equation (94–97) are respectively:

$$\begin{aligned}
&\frac{1}{2}\frac{\partial u_{11}}{\partial \bar{t}} - \frac{\mathrm{i}}{2}u_{12} + \frac{1}{2}\frac{\partial u_{10}}{\partial \bar{x}}U + \frac{\mathrm{i}}{2}u_{11}U + \frac{1}{2}\frac{\partial u_{10}}{\partial \bar{y}}V + \frac{1}{2}v_{11}\frac{\partial U}{\partial y} - \frac{\mathrm{i}}{4}u_{20}u_{10}^* \\
&\quad + \frac{\mathrm{i}}{2}u_{10}^* u_{20} + \frac{1}{4}w_{20}\frac{\partial u_{10}^*}{\partial z} + \frac{1}{4}w_{10}^*\frac{\partial u_{20}}{\partial z} + \frac{1}{2}u_{10}\frac{\partial U}{\partial x} \\
&\quad = -\frac{1}{2}\frac{\partial p_{11}}{\partial \bar{x}} - \frac{\mathrm{i}}{2}p_{12} \qquad (141)\\
&\frac{1}{2}\frac{\partial v_{11}}{\partial \bar{t}} - \frac{\mathrm{i}}{2}v_{12} + \frac{1}{2}\frac{\partial v_{10}}{\partial \bar{x}}U + \frac{\mathrm{i}}{2}v_{11}U + \frac{1}{2}\frac{\partial v_{10}}{\partial \bar{y}}V + \frac{1}{2}v_{11}\frac{\partial V}{\partial y} + \frac{1}{2}u_{10}\frac{\partial V}{\partial x} \\
&\quad - \frac{\mathrm{i}}{4}u_{20}v_{10}^* + \frac{\mathrm{i}}{2}u_{10}^* v_{20} + \frac{1}{4}w_{20}\frac{\partial v_{10}^*}{\partial z} + \frac{1}{4}w_{10}^*\frac{\partial v_{20}}{\partial z} = -\frac{1}{2}\frac{\partial p_{11}}{\partial \bar{y}} \qquad (142)\\
&\frac{1}{2}\frac{\partial w_{11}}{\partial \bar{t}} - \frac{\mathrm{i}}{2}w_{12} + \frac{1}{2}\frac{\partial w_{10}}{\partial \bar{x}}U + \frac{\mathrm{i}}{2}w_{11}U + \frac{1}{2}\frac{\partial w_{10}}{\partial \bar{y}}V - \frac{\mathrm{i}}{4}u_{20}w_{10}^* \\
&\quad + \frac{\mathrm{i}}{2}u_{10}^* w_{20} + \frac{1}{4}w_{20}\frac{\partial w_{10}^*}{\partial z} + \frac{1}{4}w_{10}^*\frac{\partial w_{20}}{\partial z} = -\frac{1}{2}\frac{\partial p_{12}}{\partial z} \qquad (143)\\
&\frac{1}{2}\frac{\partial B_{11}}{\partial \bar{t}} - \frac{\mathrm{i}}{2}B_{12} - \frac{\mathrm{i}}{4}u_{20}\Big|_{z=0}B_{10}^* + \frac{\mathrm{i}}{2}u_{10}^*\Big|_{z=0}B_{20} \\
&\quad + \frac{1}{2}\frac{\partial B_{10}}{\partial \bar{x}}U + \frac{\mathrm{i}}{2}B_{11}U + \frac{1}{2}\frac{\partial B_{10}}{\partial \bar{y}}V + \frac{1}{2}v_{10}\Big|_{z=0}\frac{\partial \zeta}{\partial y} \\
&\quad - \frac{\mathrm{i}}{8}|B_{10}|^2\frac{\partial u_{10}}{\partial z}\Big|_{z=0} + \frac{\mathrm{i}}{8}B_{10}^2\frac{\partial u_{10}^*}{\partial z}\Big|_{z=0} + \frac{\mathrm{i}}{8}|B_{10}|^2\frac{\partial u_{10}}{\partial z}\Big|_{z=0} \\
&\quad = \frac{1}{2}w_{12}\Big|_{z=0} + \frac{1}{4}B_{20}\frac{\partial w_{10}^*}{\partial z}\Big|_{z=0} + \frac{1}{2}B_{10}^*\frac{\partial w_{20}}{\partial z}\Big|_{z=0} + \frac{1}{2}\zeta\frac{\partial w_{10}}{\partial z}\Big|_{z=0} \\
&\qquad + \frac{1}{16}B_{10}^2\frac{\partial w_{10}^*}{\partial z}\Big|_{z=0} + \frac{1}{8}|B_{10}|^2\frac{\partial^2 w_{10}}{\partial z^2}\Big|_{z=0} \qquad (144)
\end{aligned}$$

Combining these equations with the results from first and second order (104–106, 115–116, 122–124, 134–135) and the solution for p_{12} (138, 140) gives the space evolution of the current modified cubic Schrödinger equation, NLSC:

$$\begin{aligned}
0 = &\frac{\partial B_{11}}{\partial \bar{x}} + 2\frac{\partial B_{11}}{\partial \bar{t}} + \mathrm{i}\frac{\partial^2 B_{10}}{\partial \bar{t}^2} - \frac{\mathrm{i}}{2}\frac{\partial^2 B_{10}}{\partial \bar{y}^2} + \mathrm{i}B_{10}^2 B_{10}^* + 2\mathrm{i}B_{11}U \\
&-6\frac{\partial B_{10}}{\partial \bar{t}}U - 5\mathrm{i}B_{10}U^2 + 2\frac{\partial B_{10}}{\partial \bar{y}}V + B_{10}\frac{\partial U}{\partial x} - \mathrm{i}\frac{\partial B_{10}}{\partial \bar{y}}\frac{\partial U}{\partial y} \qquad (145)
\end{aligned}$$

And the time evolution:

$$\begin{aligned}
0 = &\frac{\partial B_{11}}{\partial \bar{t}} + \frac{1}{2}\frac{\partial B_{11}}{\partial \bar{x}} + \frac{\mathrm{i}}{8}\frac{\partial^2 B_{10}}{\partial \bar{x}^2} - \frac{\mathrm{i}}{4}\frac{\partial^2 B_{10}}{\partial \bar{y}^2} + \frac{\mathrm{i}}{2}B_{10}^2 B_{10}^* \\
&+\mathrm{i}B_{11}U + \frac{\partial B_{10}}{\partial \bar{x}}U - \frac{\partial B_{10}}{\partial \bar{y}}V + \frac{1}{2}B_{10}\frac{\partial U}{\partial x} - \frac{i}{2}\frac{\partial B_{10}}{\partial \bar{y}}\frac{\partial U}{\partial y} \qquad (146)
\end{aligned}$$

3.2.4 Summary

In the following $B = B_1$ to simplify the notation.

Space evolution The space evolution of the current modified nonlinear Schrödinger equation which allows vorticity to the first order of ϵ, NLSC is:

$$\frac{\partial B}{\partial \bar{x}} = (\mathcal{L} + \mathcal{C} + \mathcal{N})B \tag{147}$$

$\mathcal{L}$ contains the linear terms with constant coefficients. $\mathcal{C}$ contains the linear terms with variable coefficients. And $\mathcal{N}$ is the nonlinear term:

$$\begin{aligned}
\mathcal{L} &= -2\frac{\partial}{\partial \bar{t}} - \mathrm{i}\frac{\partial^2}{\partial \bar{t}^2} + \frac{\mathrm{i}}{2}\frac{\partial^2}{\partial \bar{y}^2} \\
\mathcal{C} &= -2\mathrm{i}U + 6U\frac{\partial}{\partial \bar{t}} + 5\mathrm{i}U^2 - 2V\frac{\partial}{\partial \bar{y}} - \frac{\partial U}{\partial x} + \mathrm{i}\frac{\partial U}{\partial y}\frac{\partial}{\partial \bar{y}} \\
\mathcal{N} &= -\mathrm{i}|B|^2
\end{aligned}$$

The vertical current component, W, the vertical derivatives of the current, $\frac{\partial \boldsymbol{V}}{\partial z}$, and the surface displacement, ζ, associated with the current, appear to the next order of the equation.

The reconstruction formulas are:

$$\begin{aligned}
\bar{\eta}, \bar{u}, \bar{v}, \bar{w} &= 0 \\
\bar{p} &= -\frac{1}{2}|B|^2\mathrm{e}^{2z} \\
B_2 &= \frac{1}{2}B^2 \\
u_1 &= B\mathrm{e}^z + \mathrm{i}\frac{\partial B}{\partial \bar{t}}\mathrm{e}^z - BU\mathrm{e}^z + 2\mathrm{i}\frac{\partial B}{\partial \bar{t}}z\mathrm{e}^z - 2BUz\mathrm{e}^z \\
v_1 &= -\mathrm{i}\frac{\partial B}{\partial \bar{y}}\mathrm{e}^z \\
w_1 &= -\mathrm{i}B\mathrm{e}^z + \frac{\partial B}{\partial \bar{t}}\mathrm{e}^z + \mathrm{i}BU\mathrm{e}^z + 2\frac{\partial B}{\partial \bar{t}}z\mathrm{e}^z + 2\mathrm{i}BUz\mathrm{e}^z \\
p_1 &= B\mathrm{e}^z + 2\mathrm{i}\frac{\partial B}{\partial \bar{t}}z\mathrm{e}^z - 2BUz\mathrm{e}^z \\
u_2, v_2, w_2, p_2 &= 0
\end{aligned}$$

Time evolution The time evolution of the current modified nonlinear Schrödinger equation which allows vorticity to the first order of ϵ, NLSC is:

$$\frac{\partial B}{\partial \bar{t}} = (\mathcal{L} + \mathcal{C} + \mathcal{N})B \tag{148}$$

where

$$\begin{aligned}
\mathcal{L} &= -\frac{1}{2}\frac{\partial}{\partial\bar{x}} - \frac{\mathrm{i}}{8}\frac{\partial^2}{\partial\bar{x}^2} + \frac{\mathrm{i}}{4}\frac{\partial^2}{\partial\bar{y}^2} \\
\mathcal{C} &= -\mathrm{i}U - U\frac{\partial}{\partial\bar{x}} + V\frac{\partial}{\partial\bar{y}} - \frac{1}{2}\frac{\partial U}{\partial x} + \frac{\mathrm{i}}{2}\frac{\partial U}{\partial y}\frac{\partial}{\partial\bar{y}} \\
\mathcal{N} &= -\frac{\mathrm{i}}{2}|B|^2
\end{aligned}$$

The reconstruction formulas are:

$$\begin{aligned}
\bar{\eta}, \bar{u}, \bar{v}, \bar{w} &= 0 \\
\bar{p} &= -\frac{1}{2}|B|^2\mathrm{e}^{2z} \\
B_2 &= \frac{1}{2}B^2 \\
u_1 &= B\mathrm{e}^z - \frac{\mathrm{i}}{2}\frac{\partial B}{\partial\bar{x}}\mathrm{e}^z - \mathrm{i}\frac{\partial B}{\partial\bar{x}}z\mathrm{e}^z \\
v_1 &= -\mathrm{i}\frac{\partial B}{\partial\bar{y}}\mathrm{e}^z \\
w_1 &= -\mathrm{i}B\mathrm{e}^z - \frac{1}{2}\frac{\partial B}{\partial\bar{x}}\mathrm{e}^z - \frac{\partial B}{\partial\bar{x}}z\mathrm{e}^z \\
p_1 &= B\mathrm{e}^z - \mathrm{i}\frac{\partial B}{\partial\bar{x}}z\mathrm{e}^z \\
u_2, v_2, w_2, p_2 &= 0
\end{aligned}$$

4 Numerical implementation

4.1 Numerical scheme

Space evolutions of current modified nonlinear Schrödinger equations, (76) and (147), may be written on the form:

$$\frac{\partial B}{\partial x} = (\mathcal{L} + \mathcal{V})B \tag{149}$$

$\mathcal{L} = \mathcal{L}(\frac{\partial}{\partial t}, \frac{\partial}{\partial y})$ contains the linear terms with constant coefficients. $\mathcal{V} = \mathcal{N} + \mathcal{C}$ contains the nonlinear term, $\mathcal{N} = \mathcal{N}(|B|^2)$, and the linear terms with variable coefficients, $\mathcal{C} = \mathcal{C}(U, V, \frac{\partial}{\partial t}, \frac{\partial}{\partial y})$.

4.1.1 Splitting scheme

The formal solution of (149) is:

$$B = \mathrm{e}^{F(x,y,t)}B_0 \tag{150}$$

where $B_0 = B|_{x=0}$ and $\frac{\partial F(x,y,t)}{\partial x} = \mathcal{L}+\mathcal{V}$. If $F = F(x,y,t)$ is weakly depending on x, (150) may be approximated by:

$$B \approx \mathrm{e}^{(\mathcal{L}+\mathcal{V})x} B_0 \tag{151}$$

The exponential function may be expanded:

$$\mathrm{e}^{(\mathcal{L}+\mathcal{V})x} = 1 + (\mathcal{L}+\mathcal{V})x + \frac{1}{2}(\mathcal{L}+\mathcal{V})^2 x^2 + \frac{1}{6}(\mathcal{L}+\mathcal{V})^3 x^3 + \cdots \tag{152}$$

In numerical simulations $\mathcal{L}B$ and $\mathcal{V}B$ may be solved separately. The accuracy of the result depends on the splitting scheme. Note that it is not necessary with a more accurate splitting scheme than the accuracy of the separate solutions.

LV–split With LV–split, $\mathrm{e}^{(\mathcal{L}+\mathcal{V})x} \approx \mathrm{e}^{\mathcal{L}x}\mathrm{e}^{\mathcal{V}x}$ which may be expanded to:

$$\mathrm{e}^{\mathcal{L}x}\mathrm{e}^{\mathcal{V}x} = 1 + (\mathcal{L}+\mathcal{V})\,x + \frac{1}{2}\left(\mathcal{L}^2 + 2\mathcal{L}\mathcal{V} + \mathcal{V}^2\right)x^2 + O(x^3) \tag{153}$$

The accuracy is of first order:

$$\mathrm{e}^{(\mathcal{L}+\mathcal{V})x} - \mathrm{e}^{\mathcal{L}x}\mathrm{e}^{\mathcal{V}x} = \frac{1}{2}(\mathcal{V}\mathcal{L} - \mathcal{L}\mathcal{V})x^2 + O(x^3) \tag{154}$$

Note that $\mathcal{V}\mathcal{L}$ do not equal $\mathcal{L}\mathcal{V}$ in all cases. An an appropriate commutator is defined by:

$$[\mathcal{V},\mathcal{L}] \equiv \mathcal{V}\mathcal{L} - \mathcal{L}\mathcal{V} \tag{155}$$

so that (154) may be written on the form:

$$\mathrm{e}^{(\mathcal{L}+\mathcal{V})x} - \mathrm{e}^{\mathcal{L}x}\mathrm{e}^{\mathcal{V}x} = \frac{1}{2}[\mathcal{V},\mathcal{L}]x^2 + O(x^3) \tag{156}$$

VLLV–split With VLLV–split, $\mathrm{e}^{(\mathcal{L}+\mathcal{V})x} \approx \mathrm{e}^{\frac{1}{2}\mathcal{V}x}\mathrm{e}^{\mathcal{L}x}\mathrm{e}^{\frac{1}{2}\mathcal{V}x}$ which may be expanded to:

$$\begin{aligned}\mathrm{e}^{\frac{1}{2}\mathcal{V}x}\mathrm{e}^{\mathcal{L}x}\mathrm{e}^{\frac{1}{2}\mathcal{V}x} = 1 &+ (\mathcal{L}+\mathcal{V})x + \frac{1}{2}\left(\mathcal{L}^2 + \mathcal{L}\mathcal{V} + \mathcal{V}\mathcal{L} + \mathcal{V}^2\right)x^2 \\ &+\left(\frac{1}{6}\mathcal{L}^3 + \frac{1}{4}\mathcal{L}^2\mathcal{V} + \frac{1}{8}\mathcal{L}\mathcal{V}^2 + \frac{1}{4}\mathcal{V}\mathcal{L}^2 + \frac{1}{4}\mathcal{V}\mathcal{L}\mathcal{V} + \frac{1}{8}\mathcal{V}^2\mathcal{L} + \frac{1}{6}\mathcal{V}^3\right)x^3 \\ &+O(x^4)\end{aligned} \tag{157}$$

This gives an accuracy of second order if $[\mathcal{V},\mathcal{L}] \neq 0$:

$$\mathrm{e}^{(\mathcal{L}+\mathcal{V})x} - \mathrm{e}^{\frac{1}{2}\mathcal{V}x}\mathrm{e}^{\mathcal{L}x}\mathrm{e}^{\frac{1}{2}\mathcal{V}x} = \frac{1}{24}\Big(2\Big[\mathcal{L},[\mathcal{V},\mathcal{L}]\Big] + \Big[[\mathcal{V},\mathcal{L}],\mathcal{V}\Big]\Big)x^3 + O(x^4) \tag{158}$$

(VLLV)^3–split With (VLLV)^3–splits, a fourth order scheme from Muslu & Erbay (2004) following McLachlan (1994) is used:

$$\mathrm{e}^{(\mathcal{L}+\mathcal{V})x} \approx \phi(\alpha x)\phi\Big((1-2\alpha)x\Big)\phi(\alpha x) \tag{159}$$

where $\phi(\chi) = \mathrm{e}^{\frac{1}{2}\mathcal{V}\chi}\mathrm{e}^{\mathcal{L}\chi}\mathrm{e}^{\frac{1}{2}\mathcal{V}\chi}$ and $\alpha = (2+2^{\frac{1}{3}}+2^{-\frac{1}{3}})/3$. This gives an accuracy of fourth order.

4.1.2 Fourier transform

Fourier transform is used to solved the linear part of (149) with constant coefficients:

$$\frac{\partial B}{\partial x} \;=\; \mathcal{L}B \tag{160}$$

The Fourier transform of (160) with respect to y and t is:

$$\frac{\partial \widehat{B}}{\partial x} \;=\; \widehat{\mathcal{L}}\widehat{B} \tag{161}$$

where $\widehat{L}$ is a complex polynomial of k_y and ω. Note that $\widehat{\frac{\partial B}{\partial y}} = ik_y\widehat{B}$ and $\widehat{\frac{\partial B}{\partial t}} = -i\omega\widehat{B}$. The exact solution of (160) is:

$$\widehat{B} \;=\; \mathrm{e}^{\widehat{\mathcal{L}}x}\widehat{B}_0 \tag{162}$$

where $\widehat{B}_0 = \widehat{B}|_{x=0}$.

The Fourier transform with respect to y and t is given by:

$$\hat{B}_{ij} = \frac{1}{MN}\sum_{m=0}^{M-1}\sum_{n=0}^{N-1} B_{mn}e^{\mathrm{i}(\Omega_j t_n - k_{yi}y_m)} \tag{163}$$

where $y_m = m\Delta y$, $t_n = n\Delta t$, $k_{yi} = i\Delta k_y$, and $\Omega_j = j\Delta\omega$.

4.1.3 Finite Difference

Runge–Kutta schemes are used to solve the nonlinear part and the linear part with variable coefficients in (149):

$$\frac{\partial B}{\partial x} \;=\; \mathcal{V}B \tag{164}$$

The Runge–Kutta scheme used ought to be of the same order as the splitting scheme.

Alternative:	a	b	α	β
A	0	1	1/2	1/2
B	1/2	1/2	1	1
C	2/3	1/3	3/2	3/2
D	1/3	2/3	3/4	3/4

Table 2: *The four alternative choices for the variables in the second order Runge–Kutta scheme.*

First order A first order Euler scheme is used for the first order splitting scheme:

$$B_{x+\triangle x} = B_x + \triangle x \mathcal{V}_x B_x \tag{165}$$

Second order A second order Runge–Kutta scheme is used for the second order splitting scheme:

$$B_{x+\triangle x} = B_x + \triangle x(ak_1 + bk_2) \tag{166}$$

where

$$\begin{aligned} k_1 &= \mathcal{V}_x B_x \\ k_2 &= \mathcal{V}_{x+\alpha x}(B_x + \beta \triangle x k_1) \end{aligned}$$

The four coefficients, a, b, α, and β, have to satisfy the following three equations:

$$a + b = 1, \qquad \alpha b = \frac{1}{2}, \qquad \beta b = \frac{1}{2} \tag{167}$$

The four alternatives in table 2 is studied. Lo & Mei (1985) used alternative A. Alternative B gives the modified Euler scheme.

Fourth order The most used set of variables on the fourth order Runge–Kutta (Gerald & Wheatley, 1994) is used with the fourth order splitting scheme:

$$B_{x+\triangle x} = B_x + \frac{1}{6}\triangle x \left(k_1 + 2k_2 + 2k_3 + k_4\right) \tag{168}$$

where

$$k_1 = \mathcal{V}_x B_x$$

$$
\begin{aligned}
k_2 &= \mathcal{V}_{x+\frac{1}{2}\triangle x}\left(B_x + \frac{1}{2}\triangle x k_1\right) \\
k_3 &= \mathcal{V}_{x+\frac{1}{2}\triangle x}\left(B_x + \frac{1}{2}\triangle x k_2\right) \\
k_4 &= \mathcal{V}_{x+\triangle x}\left(B_x + \triangle x k_3\right)
\end{aligned}
$$

4.2 Model setup

The space evolution of the current modified nonlinear cubic Schrödinger equation which allows vorticity, NLSC, (147), is simulated. Test simulations are performed in order to study the effect of the different terms (see section 5.3).

The length of the time series are $T = 2000$. Using $N = 1024$ nodes, the time step is $\Delta t = \frac{T}{N} \approx 1.95$ and $\triangle\omega = \frac{2\pi}{T} \approx 0.0031$. The width of the simulation area, $y = [-20, 20]$, with 16 nodes, gives $\triangle y = 2.5$ and $\triangle k_y \approx 0.079$. Test simulations are performed with different widths (see section 5.2).

4.2.1 Incoming waves

Unidirectional incoming waves with initial Gaussian spectrum have been studied. The Fourier amplitudes at $x = 0$ are given by:

$$
\hat{B}_j = \epsilon\sqrt{\frac{\triangle\omega}{\sqrt{2\pi}\sigma_\omega}}\mathrm{e}^{-\frac{\Omega_j^2}{4\sigma_\omega^2}+\mathrm{i}\psi_j} \tag{169}
$$

The frequency is given by $\omega_j = 1 + \Omega_j$. The phases, $\psi_{i,j}$, are statistically independent and uniformly distributed on the interval $[0, 2\pi)$. We have chosen $\epsilon = 0.1$. $\sigma_\omega = 0.1$ is the bandwidth in Fourier space.

Test simulations with an incoming Stokes wave are also performed (see sections 5.2 and 5.4).

4.2.2 Current field

The NLSC equation may be used for a large range of prescribed currents. Here we have chosen two types; a surface current jet given by:

$$
U = \begin{cases} 0 & \text{when } x \le X \text{ and/or } |y| \ge Y \\ U_0 \sin^2\left(\frac{\pi}{2\triangle X}(x - X)\right)\cos^2\left(\frac{\pi y}{2Y}\right) & \text{when } x > X \text{ and } x < X + \triangle X \\ U_0 \cos^2\left(\frac{\pi y}{2Y}\right) & \text{when } x \ge X + \triangle X \end{cases} \tag{170}
$$

and a transversally uniform current given by:

$$U = \begin{cases} 0 & \text{when } x \leq X \\ U_0 \sin^2\left(\frac{\pi}{2\triangle X}(x-X)\right) & \text{when } x > X \text{ and } x < X + \triangle X \\ U_0 & \text{when } x \geq X + \triangle X \end{cases} \quad (171)$$

The wave field is allowed about 32 wavelengths, $x = [0, X)$ where $X = 200$, to develop before the waves encounter a current. $Y = 10$ is half the width of the jet. And $\triangle X = 100$ is the current build–up length. Test simulations with different build–up lengths and widths of the jet are performed (see sections 5.7 and 5.6).

We have studied three current cases: no current, co–current with $U_0 = 0.05$, and opposing current with $U_0 = -0.05$ which is not enough to reflect the waves, but sufficient to study the characteristic features of opposing currents. Test simulations are performed with other current strengths (see section 5.5).

Simulations and observations of tidal currents suggest that establishing current jets are more fanned in than terminating current jets are fanned out (Hjelmervik *et al.*, 2005, 2008). Test simulations show that the current across the jet, V, needed to satisfy the continuity equation, has negligible impact on the results and may thus be set to zero in the NLSC equation (see section 5.4). Alternatively, the continuity equation can be satisfied by a vertical current, W, which does not appear within the truncation level of the NLSC equation.

4.3 Numerical order

Here the order of different schemes with and without currents is studied.

4.3.1 Transversally uniform currents

The transversally uniform current is given by (171) with $U_0 = 0$, 0.05, and -0.05. The incoming waves are unidirectional and given by (169). The incoming phase is randomised in the same way in all simulations. The distributions of η and $|B|$ at $x = 0$ are shown in figure 4.

Time series of the envelope, B, at $x = 900$ from simulation j is used to calculate the error:

$$E_j = |B|_j - |B|_{ref} \quad (172)$$

The results with the smallest step, $\triangle x = 0.001$, is used as the reference solution. Simulations which broke down earlier than $x = 900$, are not considered.

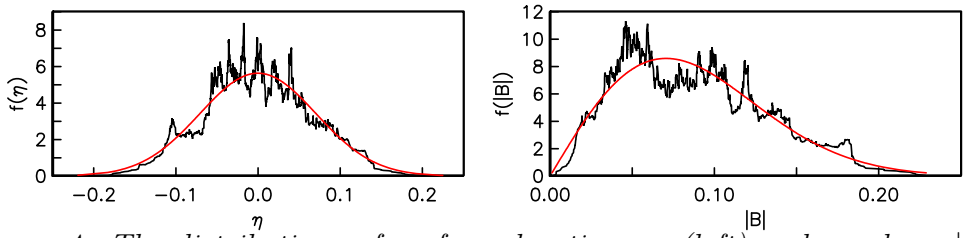

Figure 4: *The distributions of surface elevation, η, (left) and envelope, $|B|$, (right) at $x = 0$ compared to a Gaussian and a Rayleigh distribution (smooth line) respectively.*

The errors, L_1 and L_2, are calculated from the following formulas:

$$L_1 = ||E_j||_1 = \int_{-\infty}^{\infty} |E_j| \mathrm{d}t \tag{173}$$

$$L_2 = ||E_j||_2 = \sqrt[2]{\int_{-\infty}^{\infty} E_j^2 \mathrm{d}t} \tag{174}$$

The simulations are of the expected order both with and without currents (figure 5). The four alternatives in table 2 give slightly different convergence rate (figure 6a).

4.3.2 Current jets

The current jet is given by (170) with $U_0 = 0$, 0.05, and -0.05. The incoming waves are unidirectional and given by (169). The incoming phase is randomised in the same way in all simulations. The distributions of η and $|B|$ at $x = 0$ are shown in figure 4.

Time series of the envelope, B, for all values of y at $x = 400$ from simulation j is used to calculate the error:

$$E_j = |B|_j - |B|_{ref} \tag{175}$$

The results with the smallest step, $\triangle x = 0.001$, used as a reference solution. Simulations which broke down earlier than $x = 400$, are not considered.

L_1 and L_2 are calculated from the following formulas:

$$L_1 = ||E_j||_1 = \int_{-\infty}^{\infty} \int_{-\infty}^{\infty} |E_j| \mathrm{d}y \, \mathrm{d}t \tag{176}$$

$$L_2 = ||E_j||_2 = \sqrt[2]{\int_{-\infty}^{\infty} \int_{-\infty}^{\infty} E_j^2 \mathrm{d}y \, \mathrm{d}t} \tag{177}$$

The simulations are of the expected order both with and without current for first and second order schemes (figure 7a). The four alternatives in table 2 give slightly different convergence rate (figure 6b).

Without any current, the simulations are of fourth order when the fourth order scheme is used (figure 7b). The current depends on x and this is probably the reason why the simulations with current diverge from fourth order when the fourth order scheme is used. The function, $F = F(x, y, t)$ in (150) might therefore be better approximated by:

$$F(x, y, t) \quad = \quad (\mathcal{L} + \mathcal{V})_0 x + \frac{1}{2} \left(\frac{\partial \mathcal{V}}{\partial U} \frac{\partial U}{\partial x} + \frac{\partial \mathcal{V}}{\partial V} \frac{\partial V}{\partial x} \right)_0 x^2 + \cdots \qquad (178)$$

New splitting schemes have to be constructed in order to improve the fourth order scheme.

In the following, the second order scheme with alternative A and an integrating step of $\triangle x = 0.2$ is used.

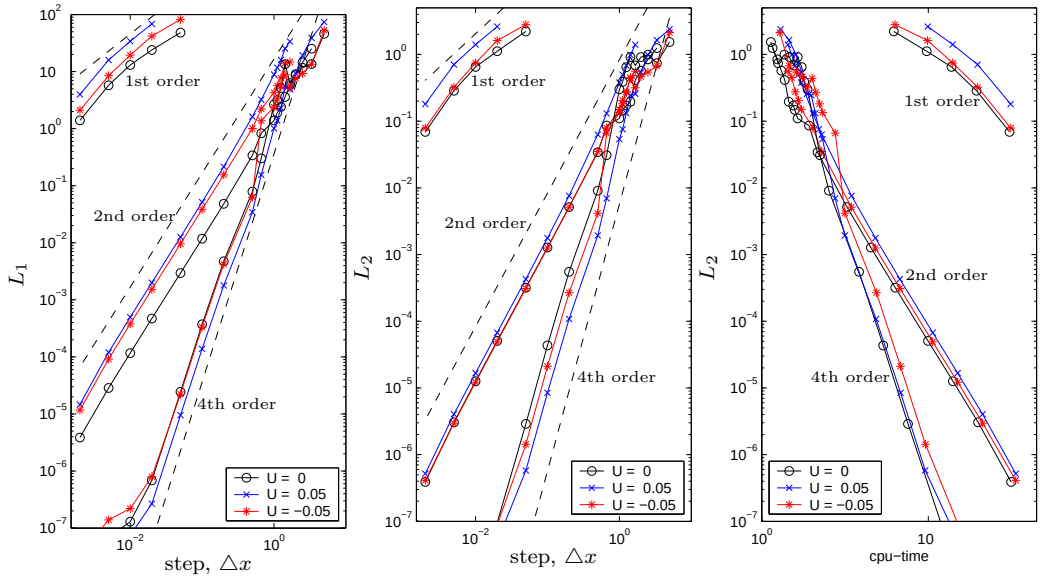

Figure 5: *The L_1 (left) and L_2 (middle) errors as a function of integrating step, $\triangle x$, and the L_2 errors as a function of cpu–time (right) for simulations with unidirectional incoming waves on transversally uniform currents. The dotted lines represent 1st, 2nd, and 4th order respectively.*

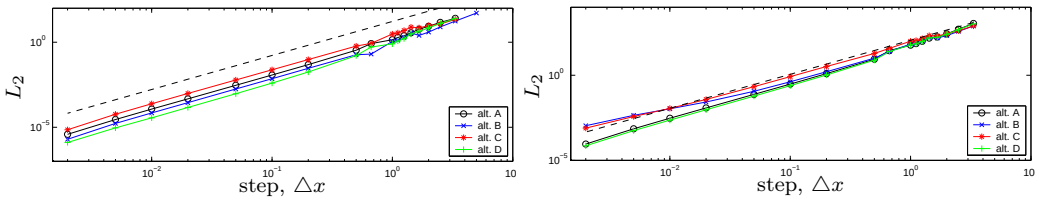

(a) no current (b) co–current jet

Figure 6: *The L_2 errors for the four alternative second order schemes. The dotted lines represent 2nd order.*

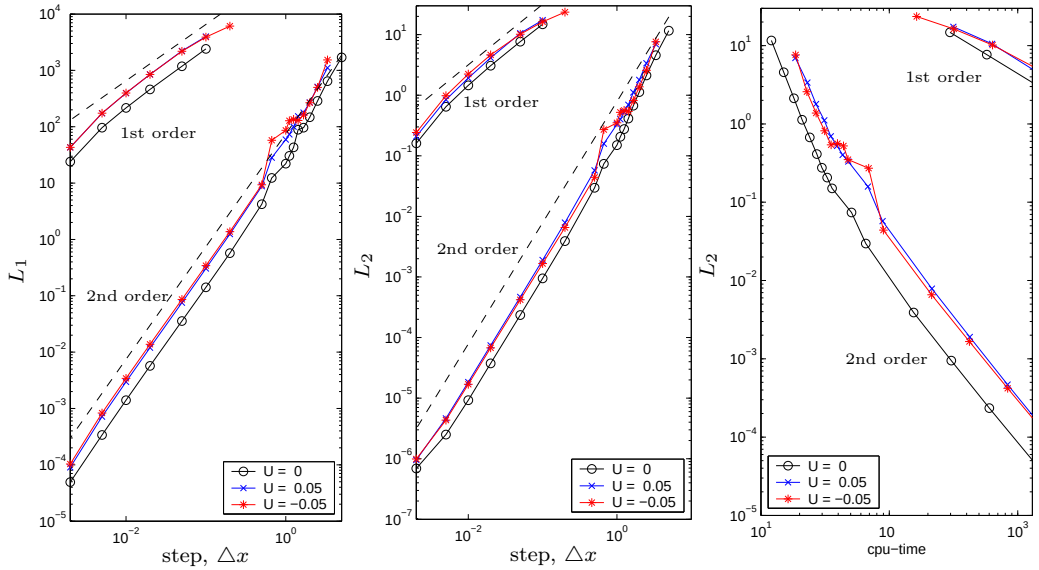

(a) 1st and 2nd order

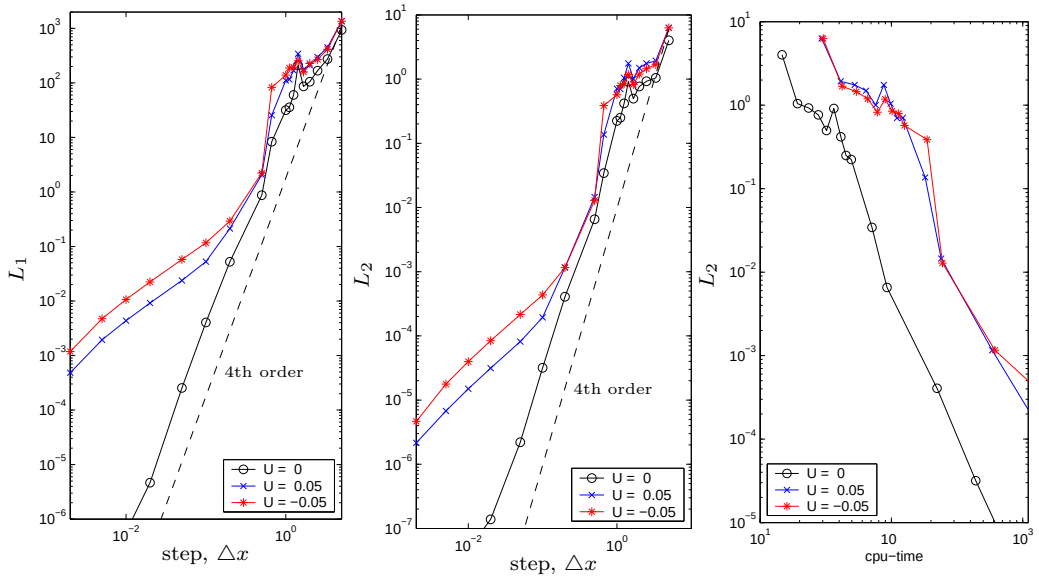

(b) 4th order

Figure 7: *The L_1 (left) and L_2 (middle) errors as a function of integrating step, $\triangle x$, and the L_2 errors as a function of cpu–time (right) for simulations with unidirectional incoming waves on current jets. The dotted lines represent 1st, 2nd, and 4th order respectively.*

5 Numerical results

A few results from simulations with the space evolution of the NLSC equation which allows vorticity, (147), will be presented. More results are published in Hjelmervik & Trulsen (2009).

The reconstruction of the surface elevation according to section 3.2, is given by:

$$\eta \;=\; \frac{1}{2}\left(B\mathrm{e}^{i(x-t)} + \frac{1}{2}\epsilon B^2\mathrm{e}^{2i(x-t)} + c.c.\right) + O(\epsilon^2) \tag{179}$$

As pointed out by Tayfun (1980) and others the second harmonic terms introduce a vertical asymmetry to the profile caused by the first harmonic terms. The crest become narrower and sharper and throughs become longer and shallower as illustrated in figure 8. Since both the envelope of the crest and the envelope of the through are displaced upward by the second harmonic terms, the distribution of wave heights remain the same. The mean value of the highest third of the wave heights – traditionally used as the significant wave height – also remains the same. The more modern definition of the significant wave height – four times the standard deviation of the surface elevation – is affected, but the change is negligible.

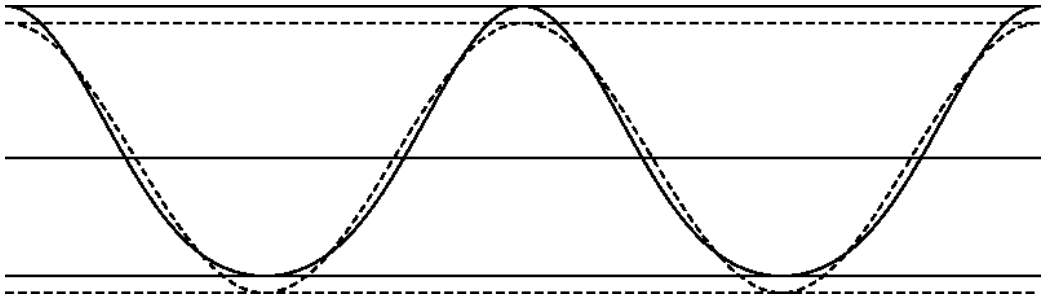

Figure 8: *An illustrative reconstruction of the surface elevation and the corresponding envelopes for fixed x or t. The dotted lines represent the first order reconstruction of (179) with $B = 0.5$. The solid lines represent the second order reconstruction which causes the crests to become narrower and sharper and the throughs to become longer and shallower. The wave heights remain unchanged.*

The first order reconstruction of the surface displacement is used to calculate both the significant wave height, H_s, and the kurtosis, κ, of the surface displacement:

$$H_s(x,y) \;=\; 4\sqrt{\overline{\eta^2}} \;=\; 4\sqrt{\frac{1}{2}\overline{|B|^2}} \tag{180}$$

$$\kappa(x,y) \;=\; \frac{\overline{\eta^4}}{\overline{\eta^2}^2} \;=\; \frac{3}{2}\frac{\overline{|B|^4}}{\overline{|B|^2}^2} \tag{181}$$

The bar represents combined time and ensemble averaging. The kurtosis equals three when the surface elevation is Gaussian distributed.

When the waves meet an opposing current, the wave height increases in the centre of the jet, and decreases at the sides of the jet. When the waves meet an co–current, the wave height decreases in the centre of the jet, and increases at the sides of the jet. The following sections show how these changes depend on the number of simulations in an ensemble (sec. 5.1), the width of the simulation area (sec. 5.2), the different terms in the NLSC equation (sec. 5.3), the transversal current (sec. 5.4), the current strength (sec. 5.5), the width of the jet (sec: 5.6), and the current build–up length (sec. 5.7).

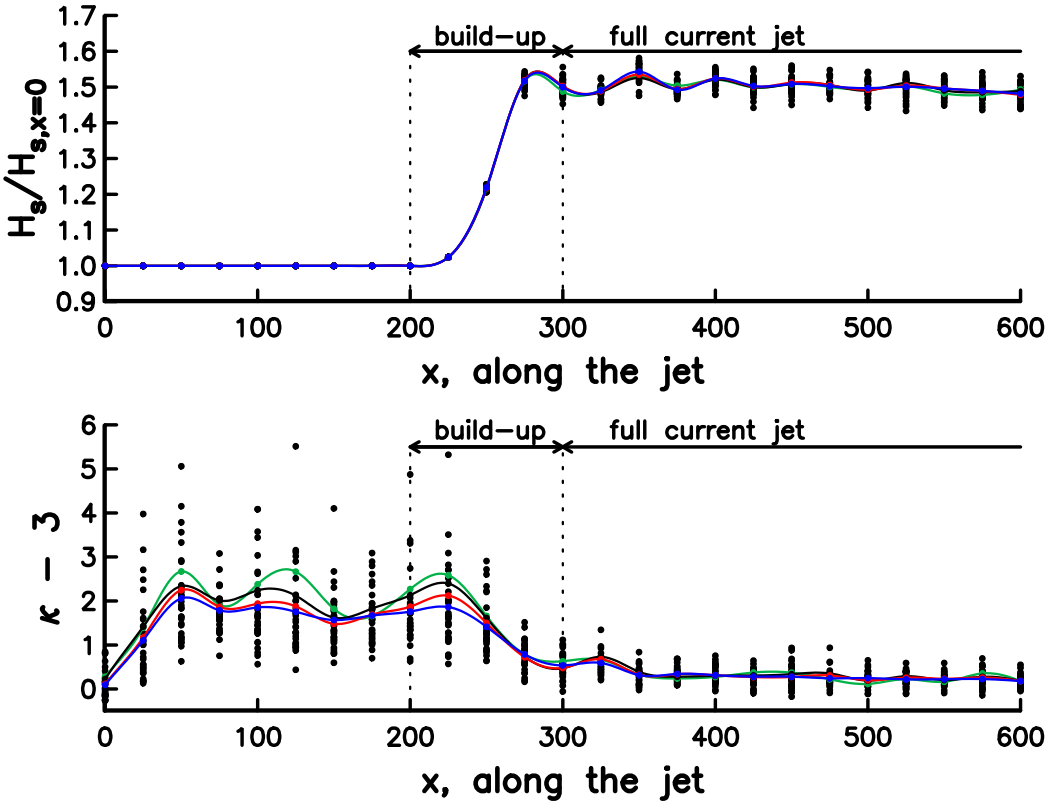

Figure 9: *The significant wave height (upper) and kurtosis (lower) from 30 single simulations (dots) and from ensembles consisting of 5 (green), 10 (black), 20 (red), and 30 (blue) simulations.*

5.1 Number of simulations in an ensemble

In order to assure statistical and numerical convergence a sufficient number of simulations should be included. Test simulations are performed with incoming unidirectional waves (169), and opposing current jet (170) with $U_0 = -0.05$.

More simulations are needed in order to calculate the kurtosis than the significant wave height (figure 9). If only the significant wave height and similar qualities are wanted, 10 simulations are sufficient. In the following we have used 30 simulations in each ensemble in order to get a more reliable result also for properties as the kurtosis.

5.2 Width of the simulation area

Test simulations are performed with different widths of the simulation area. The current jet is kept narrow ($|y| < 10$). The incoming wave is a Stokes wave. Simulations are performed with both a co–current with $U_0 = 0.05$ and an opposing current jet with $U_0 = -0.05$.

When the waves encounter a co–current jet, the amplitudes decrease in the centre of the jet and increase at the sides of the jet. The high amplitudes created at the sides of the jet, propagate away from the jet towards the simulation borders and seem to be reflected there (figure 10). When the width of the simulation area is $|y| < 40$, the high amplitudes are not reflected before $x = 375$. The amplitude in the centre of the jet seems to be periodic with a length that depends on the width of the simulation area.

When the waves encounter an opposing current jet, the amplitudes increase in the centre of the jet and decrease at the sides of the jet. The amplitude of the waves are affected only in a narrow area limited by the current jet (figure 11). The amplitude in the centre of the jet seems to be periodic with a length that does not depend on the width of the simulation area as long as the simulation area is wider than the width of the jet.

The fact that the waves converge and diverge when encountering currents, makes it possible to create very beautiful plots of the surface elevation. Heller (2005) published an art plot in an electronic art and animation catalog.

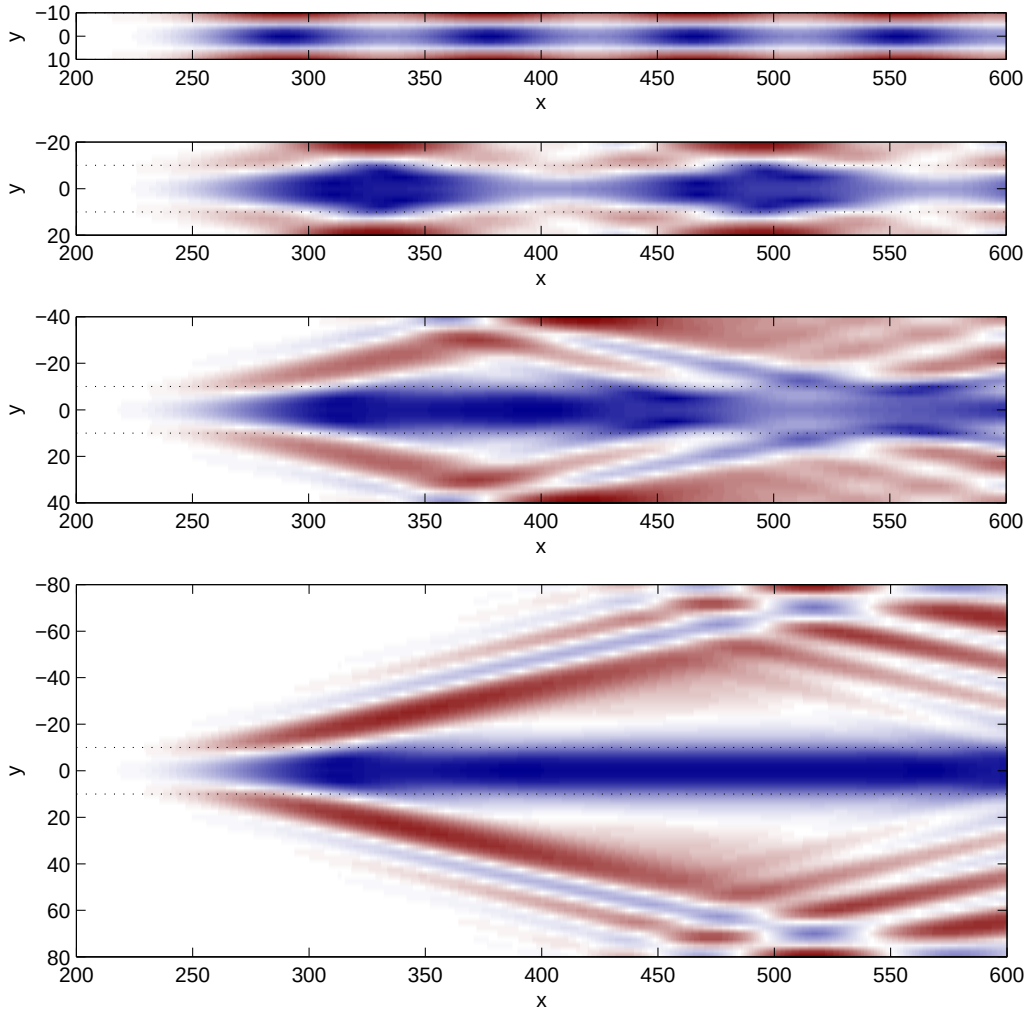

Figure 10: $|B|$ *on a co–current when* $y < 10$ *(upper),* $|y| < 20$, $|y| < 40$, *and* $|y| < 80$ *(lower). Nonlinear. Red is high values, blue small. The dotted lines mark the region of the jet.*

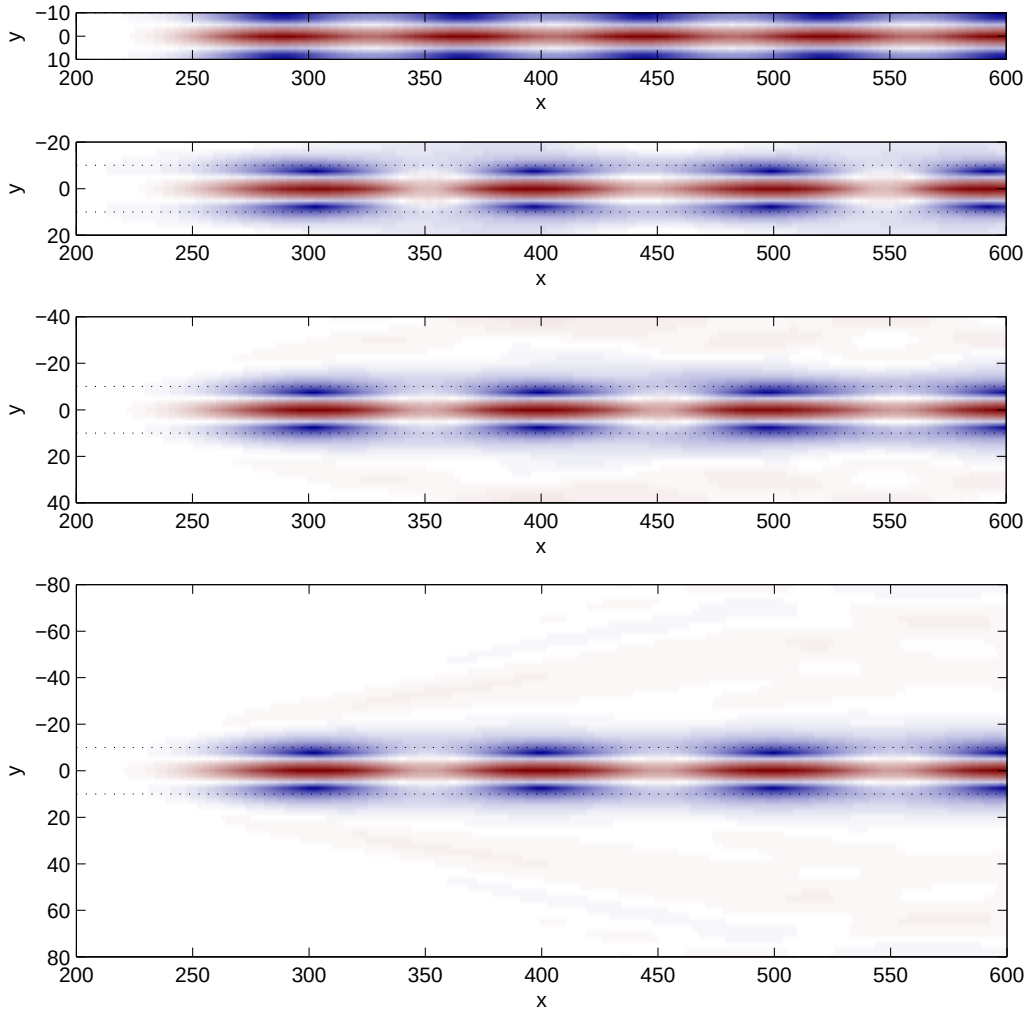

Figure 11: $|B|$ *on a counter current when* $y < 10$ *(upper),* $|y| < 20$*,* $|y| < 40$*, and* $|y| < 80$ *(lower). Nonlinear. Red is high values, blue small. The dotted lines mark the region of the jet.*

5.3 Current terms

To study the effect of the different current terms, the NLSC equation which allows vorticity (147) is simulated without one term at the time. For comparison, also the nonlinear term is left out. The simulations are performed both with a co–current and a counter current jet (170). The simulation area is given by $|y| < 20$. The incoming waves are unidirectional (169). The result for significant wave height and kurtosis is shown in figure 12 and 13.

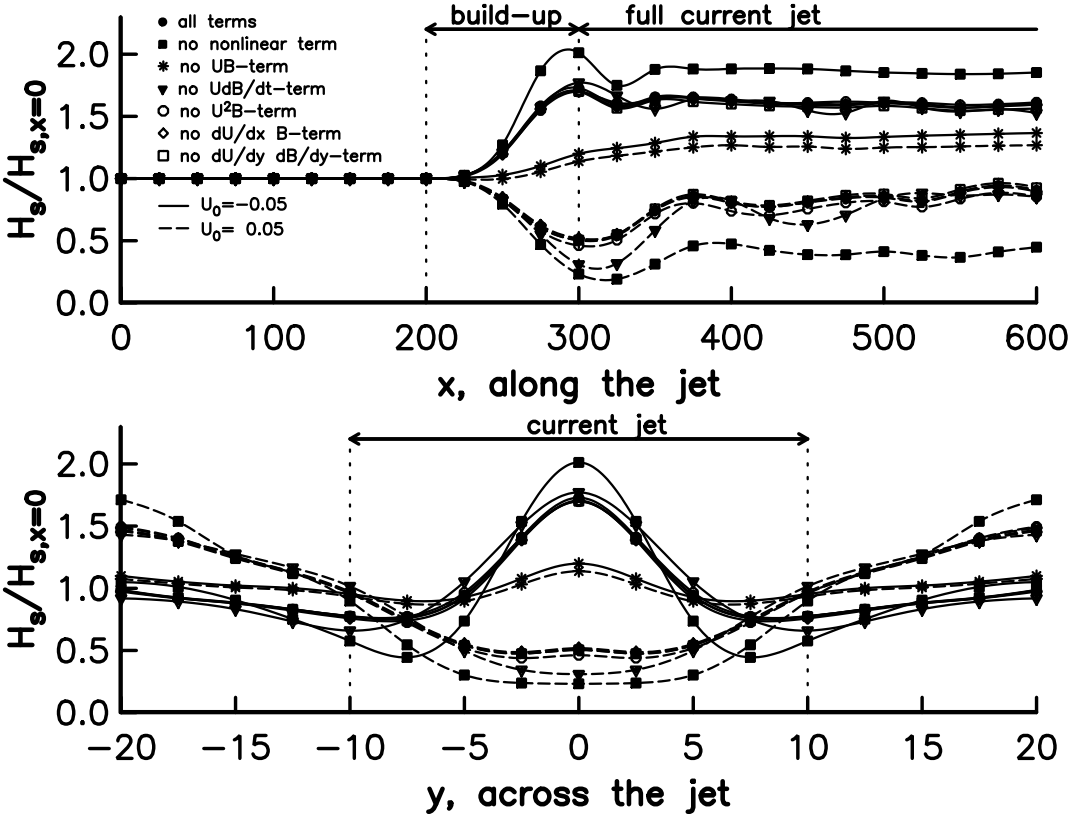

Figure 12: *The significant wave height in the centre of the jet (upper) and across the jet at $x = 300$ (lower) for unidirectional incoming waves when one term at the time is left out in the simulations.*

In linear simulations the variation in significant wave height is larger than in nonlinear simulations, and the kurtosis is close to three. Among the current terms, the UB–term has the largest impact on the results. This is not surprising since it is of lower order than the rest of the current terms. The UB–term is responsible for most of the refraction. The $U\frac{\partial B}{\partial t}$ has small impact on the significant wave height, but decreases the variation in kurtosis.

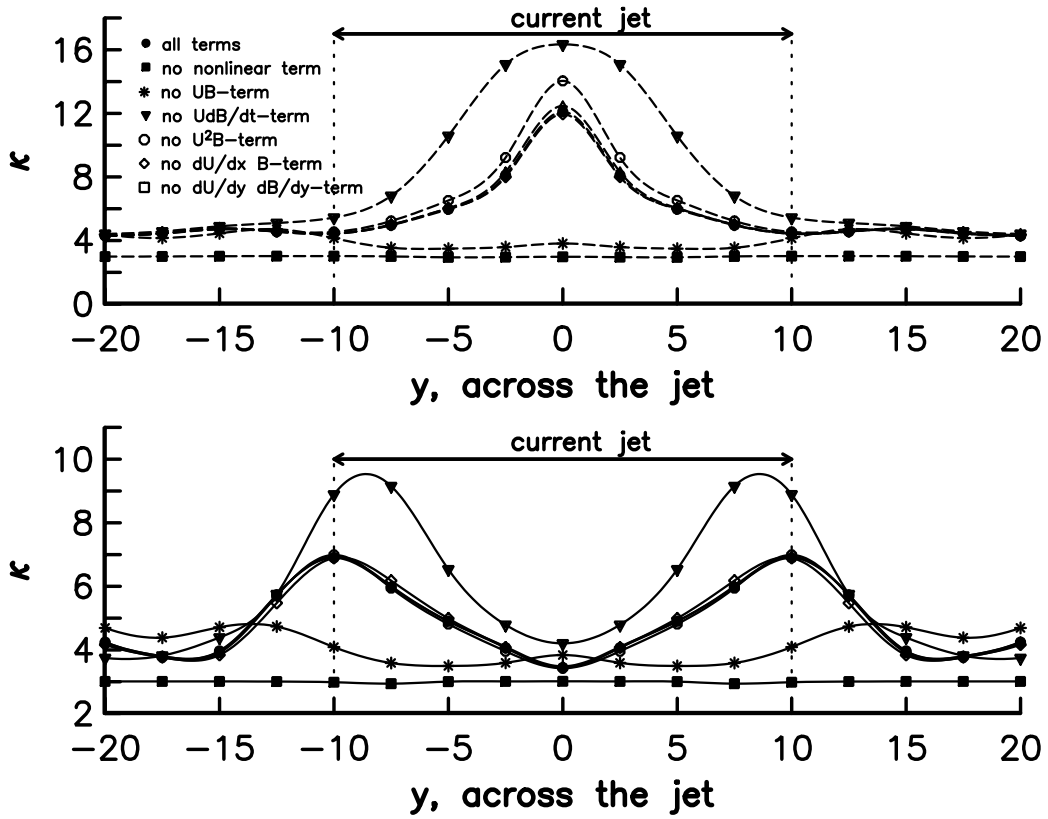

Figure 13: *The kurtosis across a co–current (upper) and counter current (lower) jet at $x = 300$ for unidirectional incoming waves when one term at the time is left out in the simulations.*

Note that the terms that do not appear in the current modified nonlinear Schrödinger equation built on potential theory, the $\frac{\partial U}{\partial y}\frac{\partial B}{\partial y}$–term and the $\frac{\partial U}{\partial x}B$–term, have small impact on the results. The U^2B–term also has minor impact. With a stronger current, these terms may have a stronger effect.

In this case, a good approximation for the NLSC equation is the simplified NLSC equation given by:

$$\frac{\partial B}{\partial x} + 2\frac{\partial B}{\partial t} + \mathrm{i}\frac{\partial^2 B}{\partial t^2} - \frac{\mathrm{i}}{2}\frac{\partial^2 B}{\partial y^2} + 2\mathrm{i}UB - 6U\frac{\partial B}{\partial t} + \mathrm{i}|B|^2 B = 0 \qquad (182)$$

Note that in Hjelmervik & Trulsen (2009) we used a different scaling of the modulation of the current normal to the principal propagation direction of the waves. This causes the $\frac{\partial U}{\partial y}\frac{\partial B}{\partial y}$–term to be left out to the truncation level of the NLSC equation.

5.4 Transversal current, V

The continuity equation for the current has to be satisfied:

$$\frac{\partial U}{\partial x} + \frac{\partial V}{\partial y} + \frac{\partial W}{\partial z} \quad = \quad 0 \tag{183}$$

During the build–up of the longitudinal current given by (170) or (171), the first term in (183) is not zero. If both the transversal current, V, and the vertical current, W, is set to zero, (183) is therefore not satisfied. Here two alternatives for the current jet is discussed. The transversally uniform current is not considered.

	$x<X$	$X < x < X + \triangle X$	$x > X + \triangle X$
$y>Y$	$U=0$ $W=0$	$U=0$ $W=0$	$U=0$ $W=0$
$\lvert y\rvert<Y$	$U=0$ $W=0$	$U=U_0 \sin^2\left(\frac{\pi}{2\triangle X}(x-X)\right)\cos^2\left(\frac{\pi y}{2Y}\right)\mathrm{e}^{-\alpha\pi z}$ $W=-U_0\frac{1}{2\alpha\triangle X}\sin\left(\frac{\pi}{\triangle X}(x-X)\right)\cos^2\left(\frac{\pi y}{2Y}\right)\mathrm{e}^{-\alpha\pi z}$	$U=U_0\cos^2\left(\frac{\pi y}{2Y}\right)$ $W=0$
$y<-Y$	$U=0$ $W=0$	$U=0$ $W=0$	$U=0$ $W=0$

Table 3: *A possible current jet when* $V = 0$.

	$x<X$	$X < x < X + \triangle X$	$x > X + \triangle X$
$y>Y$	$U=0$ $V=0$	$U=0$ $V=-U_0\frac{\pi Y}{4\triangle X}\sin\left(\frac{\pi}{\triangle X}(x-X)\right)$	$U=0$ $V=0$
$\lvert y\rvert<Y$	$U=0$ $V=0$	$U=U_0\sin^2\left(\frac{\pi}{2\triangle X}(x-X)\right)\cos^2\left(\frac{\pi y}{2Y}\right)$ $V=-U_0\frac{Y}{4\triangle X}\sin\left(\frac{\pi}{\triangle X}(x-X)\right)\left(\cos\left(\frac{\pi y}{Y}\right)+\frac{\pi y}{Y}\right)$	$U=U_0\cos^2\left(\frac{\pi y}{2Y}\right)$ $V=0$
$y<-Y$	$U=0$ $V=0$	$U=0$ $V=U_0\frac{\pi Y}{4\triangle X}\sin\left(\frac{\pi}{\triangle X}(x-X)\right)$	$U=0$ $V=0$

Table 4: *A possible current jet when* $W = 0$.

At one extreme, the transversal current is set to zero. A possible current jet is then given in table 3. The parameter α tells how quickly the current decrease towards the bottom. If the scaling in section 3.1 or 3.2 is applied, α has to be less than 0.05. The vertical current first appears in the current modified Schrödinger equation to Dysthe level, and is not implemented in numerical models for cubic Schrödinger equations.

At the other extreme, the vertical current is set to zero. A possible current jet is then given in table 4. A few simulations are performed with the current

jet given in table 4. The incoming wave is a Stokes wave. Both linear and nonlinear simulations are performed with both a co–current with $U_0 = 0.05$ and an opposing current with $U_0 = -0.05$. The results are compared with results from simulations with $V = 0$. The transversal current has little effect in all simulations. The effect on the envelope is shown in figures 14–15.

To assume that both the vertical and the transversal currents equal zero, seems to be a good approximation in this case.

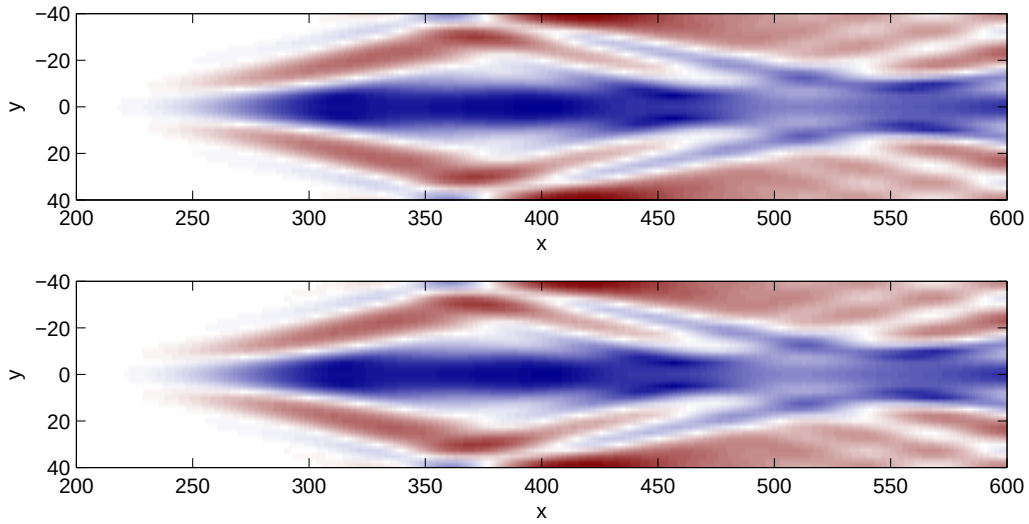

Figure 14: $|B|$ *on a co–current with* $V = 0$ *(upper) and* $V \neq 0$ *(lower). High values are red, small values are blue.*

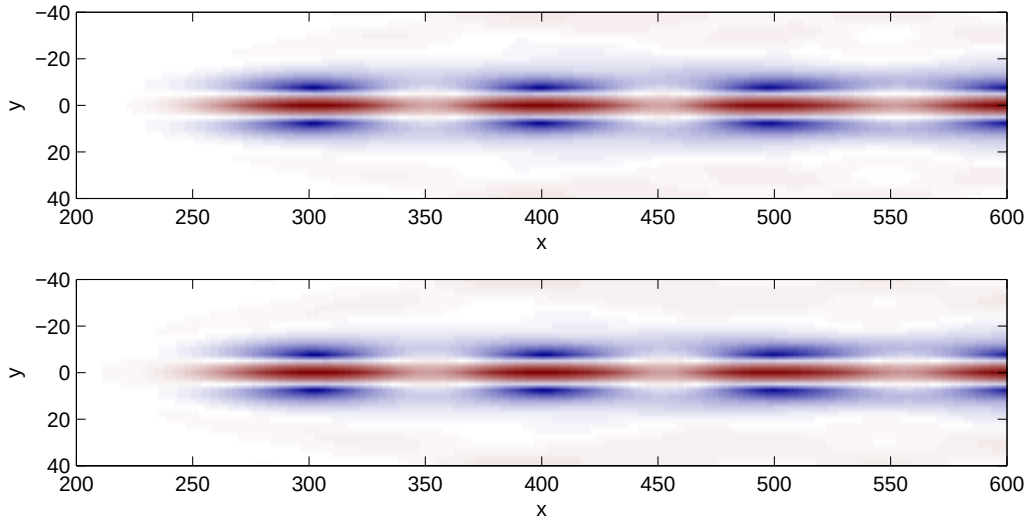

Figure 15: $|B|$ *on a counter current with* $V = 0$ *(upper) and* $V \neq 0$ *(lower). High values are red, small values are blue.*

5.5 Current strength

Test simulations are performed with different strengths of the current jet, (170). The simulation area is given by $|y| < 20$ The incoming waves are unidirectional (169).

The significant wave height in the centre of the jet increases with increasing strength of the opposing current jet, and decreases with increasing strength of the co-current (figure 16). The significant wave height seems to oscillate with a period depending on the strength of the current jet.

Note that in the derivation of the Schrödinger equations, U_0 is assumed of order ϵ. The spectrum is not narrow banded when $|U_0| = 0.25$, and the simulations seem to break down when $|U_0| > 0.25$. On counter currents this may be due to longitudinal refraction. When $\mathbf{U} = U(x)\mathbf{i}$ the dimensionless stopping velocity is $U = -\frac{1}{4}$ according to (7) and linear ray theory (Peregrine & Smith, 1979).

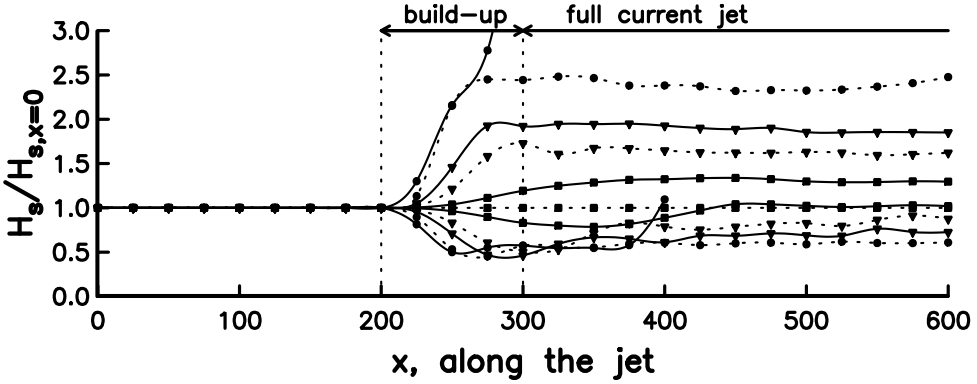

Figure 16: *The significant wave height of waves in the centre of current jets with different strengths:* $|U_0| = 0$ *(square, dotted), 0.01 (square, solid), 0.05 (triangle, dotted), 0.10 (triangle, solid), 0.25 (disk, dotted), and 0.50 (disk, solid).*

5.6 Width of the jet

Test simulations are performed with different widths, Y, of the current jet (170). The simulation area is given by $|y| < 40$ The incoming waves are unidirectional (169). Simulations are performed with both a co–current and an opposing current jet.

The significant wave height along the centre of the jet and across the jet changes more slowly the wider the jet is (figure 17). On an opposing current jet, the significant wave height does not depend on the width of the jet when

the waves are adjusted to the current jet. When the width of the jet equals the width of the simulation area, oscillations occur due to channel effects.

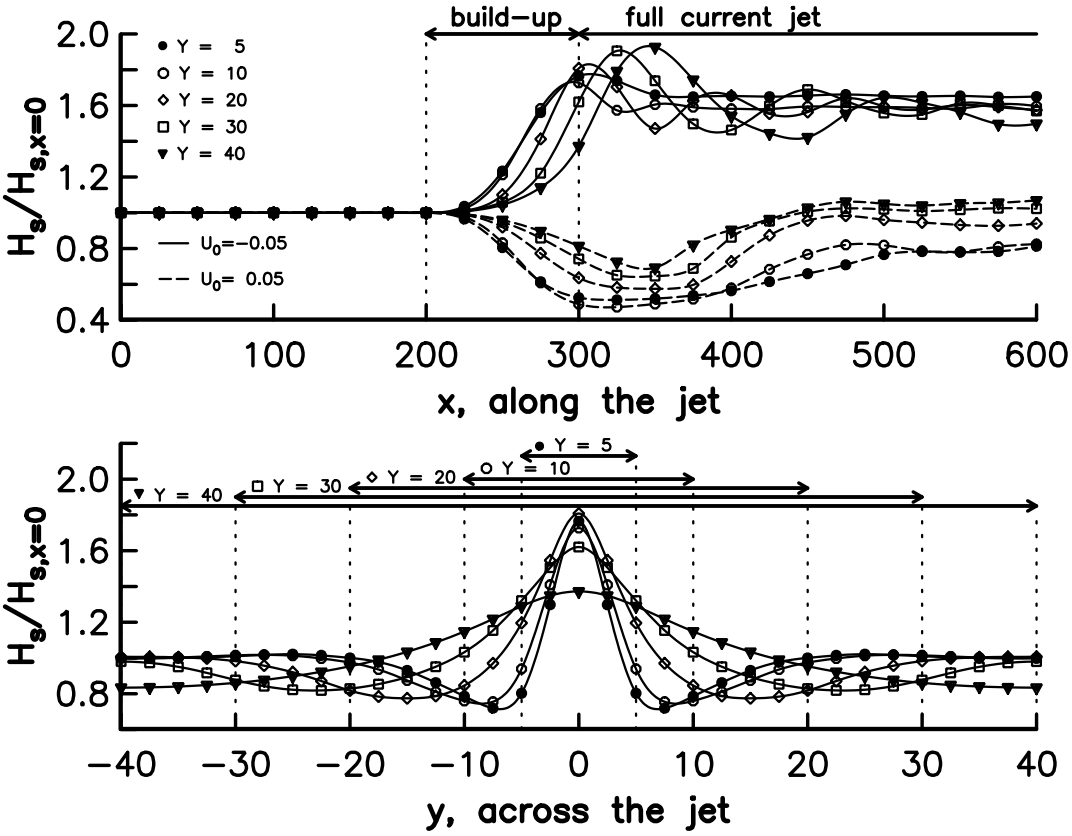

Figure 17: *The significant wave height in the centre of a co–current and a counter current jet (upper) and across a counter current jet at x=300 (lower) with different widths of the jet.*

5.7 Build–up length

Test simulations are performed with different build–up lengths, $\triangle X$, of the current jet, (170). The simulation area is given by $|y| < 40$ The incoming waves are unidirectional (169).

Both the significant wave height and the kurtosis in the centre of the jet change quicker with shorter build–up lengths (figure 18). On opposing current jets the significant wave height seems to oscillate more with shorter build–up lengths, but stabilises around the same value after the build–up independent of the build–up length. The kurtosis decreases more quickly with shorter build–up lengths of opposing jets. On co–current jets channel

effects are more pronounced for shorter build–up lengths due to a stronger divergence during the build–up. The kurtosis increases quicker and reaches a larger maximum with shorter build–up lengths of the co–current.

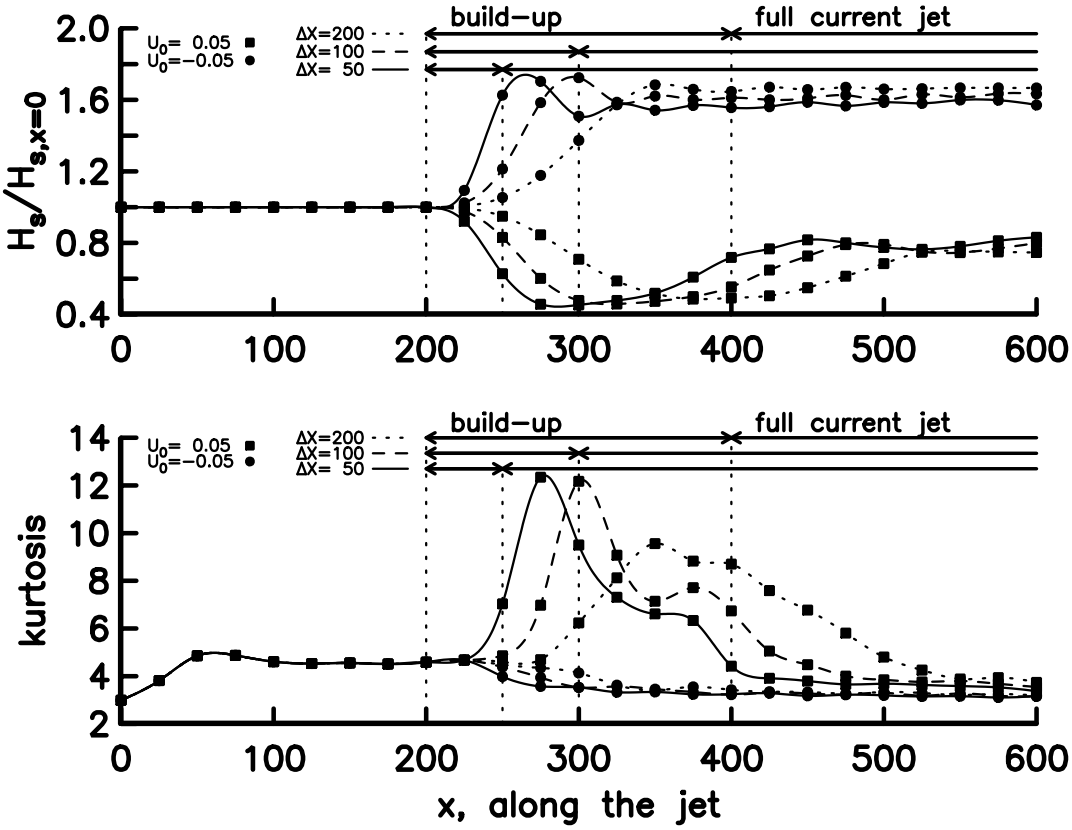

Figure 18: *The significant wave height (upper) and kurtosis (lower) of waves in the centre of current jets with different build–up lengths.*

6 Conclusion

Two new current modified Schrödinger equations have been derived; one using potential theory, and one allowing vorticity (NLSC). The splitting schemes are described and the corresponding numerical orders tested. Since the current is inhomogeneous, new fourth order splitting schemes should be constructed.

Monte–Carlo simulations are performed to estimate statistical wave properties. 30 simulations in each ensemble is found to be sufficient to assure statistical and numerical convergence for higher order properties as the kurtosis. Different model setups are studied. When waves encounter a counter current, the simulation area should be wider than twice the width of the jet.

To study the effect of each current term in the NLSC equation, simulations are performed without one term at the time. It is found that the current term to linear order contains most of the refraction. The nonlinear term has larger impact than the rest of the current terms. The contribution from the transversal current required to satisfy the continuity equation for the current, is shown to be negligible for waves on collinear jets.

The statistical wave properties are also used to illustrate different current jet configurations. If the strength of the counter current jet is increased, the wave height increases and seems to oscillate with a period depending on the strength of the jet. After the waves are adjusted to a counter current, the significant wave height does not seem to depend on neither the width nor the build–up length of the jet.

The current modified Schrödinger equation and model setup presented here are expected to have a large range of application possibilities. The occurrence of freak waves on collinear currents is discussed in Hjelmervik & Trulsen (2009).

Here only collinear currents are studied. The transversal current is assumed at the same strength as the longitudinal current in the derivation of the current modified nonlinear Schrödinger equation which allows vorticity. Thereby the equation may be used for oblique waves on current jets.

The current modified nonlinear Schrödinger equation for potential currents is derived to Dysthe level. It can easily be implemented in the numerical model. And the results are expected to be interesting. Schrödinger equations to Dysthe level are known to lower the kurtosis.

References

Bottin, R. R. Jr. & Thompson, E. F. 2002 Comparisons of physical and numerical model wave predictions with prototype data at Morro Bay harbor entrance, California. *U. S. Army Engineer.*

Davey, A. & Stewartson, K. 1974 On three-dimensional packets of surface waves. *Proc. R. Soc. Lond.* A **338**, 101–110.

Dysthe, K. B. 1979 Note on the modification to the nonlinear Schrödinger equation for application to deep water waves. *Proc. R. Soc. Lond. A* **369**, 105–114.

Dysthe, K. B. & Das, K. P. 1981 Coupling between a surface-wave spectrum and an internal wave: modulational interaction. *J. Fluid Mech.*, **104**, 483-503.

Forristall, G. 1978 On the statistical distribution of wave heights in a storm. *J. Geophys. Res.* **83** 8C5), 2353–2358.

Gerald, C. F. & Wheatley, P. O. 1994 Applied Numercial Analysis - Fifth edition. *Addison-Wesley Publishing company, Inc.*

Gerber, M. 1987 The Benjamin-Feir instability of a deep water Stokes wavepacket in the presence of a non-uniform medium. *J. Fluid Mech.* **176**, 311–332.

González, F. I. 1984 A case study of wave-current-bathymetry interactions at the Columbia river entrance. *J. Phys. Oceanogr.* **14**, 1065–1078.

Hasimoto, H. & Ono, H. 1972 Nonlinear modulation of gravity waves. *J. Phys. Soc. Japan.* **33**, 805–811.

Heller, E. 2005 Eric Heller. In *ACM SIGGRAPH 2005 Electronic Art and Animation Catalog* (Los Angeles, California, August 01 - 04, 2005). SIGGRAPH '05. ACM, New York, NY, 78-79.

Hjelmervik, K., Ommundsen, A. & Gjevik, B. 2005 Implementation of non-linear advection terms in a high resolution tidal model. *University of Oslo, preprint.*

Hjelmervik, K., Lynge, B. K., Ommundsen, A. & Gjevik, B. 2008 Interaction of tides and storm surges in the Tjeldsunet channel in northern Norway. *Ocean Dynamics* (submitted).

Hjelmervik, K. & Trulsen, K 2008 Freak wave statistics on collinear currents *J. Fluid Mech.* (submitted).

Jonsson, I. G. 1990 Wave-current interactions. In *The Sea, Ocean Eng. Sci.* (ed. by B. Le Méhauté & D. M. Hanes), pp. 65–120, Wiley-Interscience, Hoboken, N. J.

Lavrenov, I. V. 1998 The wave energy concentration at the Agulhas current off South Africa. *Natural Hazards* **17**, 117–127.

Lavrenov, I. V. & Porubov, A. V. 2006 Three reasons for freak wave generation in the non-uniform current. *Eur. J. Mech. B/Fluids* **25**, 574–585.

Lo, E. Y. & Mei, C. C. 1985 A numerical study of water-wave modulation based on a higher-order nonlinear Schrödinger equation. *J. Fluid Mech.* **150**, 395–416.

Longuet-Higgins, M. S. & Stewart, R. W. 1961 The changes in amplitude of short gravity waves on steady non-uniform currents. *J. Fluid Mech.* **10**, 529–549.

MacIver R. D., Simons, R. R. & Thomas, G. P. 2006 Gravity waves interacting with narrow jet-like current. *J. Geophys. Res.* **111**, C03009.

MacMahan, J. H., Thornton, E. B. & Reniers, A. J. H. M. 2006 Rip current review. *Coastal Engineering* **53**, 191–208.

McLachlan, R. 1994 Sympletic integration of Hamiltonian wave equation. *Numer. Math.* **66** 465.

Mei, C. C. 1989 The applied Dynamics of ocean surface waves. *World Scientific Publishing Co., Singapore.*, ISBN 9971-50-789-7

Mori, N., Liu, P. C. & Yasuda, T. 2002 Analysis of freak wave measurements in the sea of Japan. *Ocean Engineering* **29**, 1399–1414.

Muslu, G. M. & Erbay, H. A. 2004 Higher-order split-step Fourier Schemes for the generalized nonlinear Schrödinger equation. *Mathematics and Computers in Simulation* **67**, 581–595.

Peregrine, D. H. 1976 Interaction of water waves and currents. *Adv. Appl. Mech.* **16**, 9–117.

Peregrine, D. H. & Smith, R. 1979 Nonlinear effects upon waves near caustics. *Phil. Trans. R. Soc. Land. A* **292**, 341–370.

Stewartson, K. 1977 On the resonant interaction between a surface wave and a weak surface current. *Mathematika* **24**, 37–49.

Stocker, J. D. & Peregrine, D. H. 1999 The current-modified nonlinear Schrödinger equation. *J. Fluid Mech.* **399**, 335–353.

Tayfun, M. A. 1980 Narrow-band nonlinear sea waves. *J. Geophys. Res.* **85**, 1548–1552.

Trulsen, K., Kliakhandler, I., Dysthe, K. B., & Velarde, M. G. 2000 On weakly nonlinear modulation of waves on deep water. *Phys. Fluids* **12**, 2432–2437.

Trulsen, K. & Mei, C. C. 1993 Double reflection of capillary/gravity wavs by a non-uniform current: a boundary–layer theory. *J. Fluid Mech.* **251**, 239–271.

Turpin, F-M., Benmoussa, C. & Mei, C. C. 1983 Efects of slowly varying depth and current on the evolution of a Stokes wavepacket. *J. Fluid Mech.* **132**, 1–23.

Weidman, J. A. C. & Herbst, B. M. 1986 Split-step methods for the solution of the nonlinear Schrödinger equation. *SIAM J. Numer. Analy.* **23**, 485–507.

White, B. S. 1999 Wave action on currents with vorticity. *J. Fluid Mech.* **386**, 329–344.

White, B. S. & Fornberg, B. 1998 On the chance of freak waves at sea. *J. Fluid Mech.* **335**, 113–138.

Yuen, H. C. & Lake, B. M. 1982 Nonlinear dynamics of deep-water gravity waves. *Adv. Appl. Mech.* **22**, 67–229.

Zakharov, V. E. 1968 Stability of periodic waves of finite amplitude on the surface of a deep fluid. *J. Appl. Mech. Tech. Phys.* **9**, 86–94.